CHAPTER

18

Geochemical and Biological Consequences of Phytoplankton Evolution

MIRIAM E. KATZ, KATJA FENNEL, AND PAUL G. FALKOWSKI

I. INTRODUCTION

The early evolution of Earth's atmosphere, oceans, and lithosphere strongly influenced, and in turn was influenced by, the evolution of life. Reconstructing the interactions and feedbacks between life and abiotic systems is one of the most challenging problems in understanding the history of the planet. Analyses of the stable isotopes of five of the six major light elements that comprise all life on Earth (H, C, N, O, and S; there is only one stable isotope of P) have provided clues about the co-evolution of life and geophysical processes on Earth. Of these, the isotopic records of carbon and sulfur are perhaps the most useful in reconstructing redox chemistry resulting from biological evolution.

Because these two elements are extremely abundant on the surface of the planet and are capable of accepting and donating four and eight electron equivalents, respectively, on geological time scales, their global biological chemistry exerts a major control on the redox conditions of the atmosphere and oceans. In this chapter, we examine the role of marine photoautotrophs on Earth's carbon cycle, with an emphasis on the impact of these organisms on the redox changes inferred from the isotopic signals preserved in the geological record.

A. The Two Carbon Cycles

There are two major carbon cycles operating on Earth. The "geological" (or "slow") carbon cycle consists of a linked set of wholly abiotic, acid-base reactions in which CO_2 is outgassed primarily via volcanism, becomes hydrated to form carbonic acid, and is subsequently consumed, primarily by reactions with magnesium- and calcium-bearing silicate rocks, to form magnesium and calcium carbonates. The cycle is completed when the carbonates are subducted along active continental margins, heated in the mantle, and outgassed again. In this cycle, no electron transfers occur and there are no significant changes in the isotopic compositions of the various carbon pools (Berner 2004). This geological carbon cycle, which is strictly dependent upon tectonic processes, operates on time scales of hundreds of millions of years; on such time scales, it is generally assumed that the balance between volcanism and weathering largely determines the CO_2 concentration in Earth's atmosphere (e.g., Berner, 1991).

The "biological" (or "fast") carbon cycle is biologically driven and is based on redox reactions, which are at the core the fundamental chemistry of life (Falkowski 2001). Redox reactions are characterized by transfers of electrons with or without protons, and like acid-base reactions, they always occur in pairs. CO_2 is a potential electron sink; in its most reduced form, it can accept up to four electrons and protons. Such reduction reactions are endergonic and do not occur spontaneously on Earth's surface without biological catalysis. The biologically catalyzed reduction of CO_2 invariably leads to the production of an oxidant. If oxygenic photosynthesis is the catalytic reaction, then H_2O is the source of the electrons and protons, and the oxidized water is converted to O_2. In the steady state, the oxidant produced by the photoautotrophs is rapidly consumed (reduced) by heterotrophs to reoxidize the organic matter. However, if some small fraction of the organic matter is buried in sediments, it can escape biological reoxidation; the buried organic matter is, in effect, a sink of reductant. Electron balance requires that if reductants are buried in the lithosphere, oxidants must be produced somewhere else; in this case, this occurs in the atmosphere and oceans (Holland 1984). Hence, burial of organic matter implies oxidation of the surface of Earth (Hayes *et al*. 1999; Hayes and Waldbauer 2006).

The biological reduction of CO_2 to form organic matter is invariably associated with a large kinetic isotopic fractionation of up to ~ 25‰. Hence, long-term burial of organic matter depletes the atmosphere and ocean of ^{12}C, resulting in ^{13}C-enriched carbonate pools (e.g., Broecker and Peng 1982; Kump and Arthur 1999). Similarly, as long-term burial of organic matter depletes the atmosphere and ocean of ^{12}C, organic matter becomes continuously enriched in ^{13}C over time. These two fractionations are the basis of the isotopic mass balance quantified as:

$$f_w * \delta^{13}C_w + f_v * \delta^{13}C_v = f_{carb} * \delta^{13}C_{carb} + f_{org} * \delta^{13}C_{org} \quad (1)$$

where f = fraction (i.e., a dimensionless ratio in which the sum of all "fs" in the equation equals 1.0), w = weathering processes, v = volcanic/hydrothermal outgassing, carb = carbonate, and org = organic carbon.

This equation is a biogeochemical analogue of the physical notion that, in the steady state, "what goes up, must come down." The left-hand side of the equation represents the input of carbon to the

atmospheric/oceanic/terrestrial ecosystems from the lithosphere, and the right-hand side represents the output of organic matter and carbonates from the ocean and land to the lithosphere. Clearly, net oxidation of Earth's atmosphere means that the equation cannot be in steady state; rather, the burial of organic carbon must exceed its oxidation in this scenario (Berner and Canfield 1989).

The average isotopic value of mantle CO_2 is ca. −5‰, whereas that of organic matter is ca. −25‰. Hence, to balance the input with the output, the ratio of buried organic carbon relative to total carbon is about 0.20 to 0.25. That is, for every one atom of carbon buried as organic matter, between four and five atoms are buried as carbonate (see Guidry *et al*., Chapter 17, this volume). Hence, changes in marine $\delta^{13}C_{carb}$ and $\delta^{13}C_{org}$ through time serve as sedimentary archives of changes in carbon sources and sinks, thereby providing the best monitor available to reconstruct the geological carbon cycle and its role in the oxidation state of the planet's surface.

B. The "Great Oxidation Event" and the Wilson Cycle

Although the evolution of oxygenic photosynthesis provided a mechanism to produce large amounts of O_2 from the ubiquitous and abundant sources of reductant (water) and energy (solar radiation), this process, in and of itself, was not sufficient to oxidize Earth's atmosphere and oceans. Net oxidation requires net long-term burial of organic carbon in the lithosphere, where it is protected from reoxidation. Let us briefly examine how this process evolved.

The two basic physical processes involved in continental evolution are the Archimedes Principle and heat conduction. The former holds that less dense bodies will float on more dense bodies; the latter suggests that thicker, more insulated bodies do not conduct heat as efficiently as thinner, less insulated bodies. Let us put these two concepts to work in understanding how tectonic processes alter continental configuration and how that, in turn, influences the carbon cycle and the oxidation state of Earth.

It is generally believed there were no continents in the early Archean Eon (Drake and Righter 2002). The growth of continents required repeated subduction of dense, basaltic mantle rocks, where heating and recrystallization in the presence of water vapor produced silicate-rich (so-called felsic) rocks such as granites. The granitic rock aggregated over time into larger units to form cratons (the large, heterogenous lithopheric bases of continents), which are lighter than the underlying mantle, and therefore float on that semifluid structure.

Cratons are thick, about three to four times thicker than the denser basalts (called mafic rocks) that form the oceanic crusts. Near Earth's surface, the heat that emanates from within the core is conducted about three times more efficiently through the thin oceanic crust than it is through the thicker continental crust. This differential heat dissipation leads to the build-up of thermal energy below large cratons, causing massive pressures beneath them. As the heat and pressure build, the craton (continent) eventually thins and fractures, and pieces of continents slowly rift apart, creating a new oceanic ridge spreading center between the continental fragments. Heat-driven convection in the mantle below the lithosphere drives the tectonic plates apart with the fragmented continents attached, and new oceanic crust forms at the intervening spreading center. The oceanic crust becomes cooler and denser as it ages and eventually subsides as it moves away from the spreading center. When this old basaltic crust becomes so dense that it subsides below the less dense adjacent continental crust, a new subduction zone is created, the whole process reverses itself, and the ocean basin is consumed as the continents ultimately reassemble. The episodic break-up, dispersal, and subsequent reassembly of supercontinents occurs over ~300–500 million year (myr) intervals

(e.g., Valentine and Moores 1974; Fischer, 1984; Rich *et al*. 1986; Worsley *et al*. 1986) and is known as the "Wilson cycle," named after its conceptual discoverer, J. Tuzo Wilson (Wilson 1966).

A critical point in the discussion of the Wilson cycle is the exchange between oceanic crust and cratons. As oceanic crust subducts along continental margins, a fraction of the oceanic material can be "shaved off" during orogenic (mountain-building) processes along the active margin. In this way, some oceanic sediments and crust can accrete onto the cratons, effectively removing these sediments from the Wilson cycle. Hence, organic matter buried on the ocean margins can be displaced onto the cratons, where it may be sequestered for hundreds of millions (and even billions) of years, even though portions of the cratons themselves are returned to the oceans via weathering of continental rocks. This process of continental accretion is critical to allowing oxidants to accumulate in the atmosphere; without cratons, the oxygen concentration on Earth would be much lower than it is at present. Hence, the net oxidation of Earth 2.3 billion years ago (Ga), known as the "Great Oxidation Event" (Holland 1997), implies that the rates of burial and sequestration of organic carbon exceeded the rates of weathering and oxidation. This process almost certainly was enabled by the formation of large cratons during this period in Earth's history. However, although the tectonic processes on Earth are absolutely essential to planetary geochemistry, like photosynthesis, tectonics alone is also insufficient to lead to a net oxidation of Earth's atmosphere and oceans. Form and function of the photoautotrophs play an integral role.

II. THE ROLE OF PHYTOPLANKTON IN THE GEOLOGICAL CARBON CYCLE

Marine phytoplankton constitute less than 1% of Earth's photosynthetic biomass today, yet they are responsible for more than 45% of our planet's annual net primary production (Field *et al*. 1998). How has primary and export production affected the carbon cycle in the past? To answer this question, we begin with a review of the macroevolutionary trends of marine phytoplankton.

A. Early Phytoplankton Evolution

The evolutionary succession of marine photoautotrophs began in the Archean Eon with the origin of photosynthesis, perhaps as early as 3.8 Ga (see Knoll *et al*., Chapter 8, this volume). Eukaryotes first appeared in the fossil record ~1800 million years ago (Ma) (Han and Runnegar 1992; Knoll 1994; Javaux *et al*. 2001), yet molecular biomarkers show that both prokaryotic cyanobacteria and eukaryotic algae evolved by 2700 Ma (Brocks *et al*. 1999; Summons *et al*. 1999), if not earlier (Knoll 2003; Knoll *et al*., Chapter 8, this volume). A schism occurred early in the evolution of eukaryotic photoautotrophs and gave rise to the two major plastid superfamilies, the "green" (chlorophyll *b*-containing) and "red" (chlorophyll *c*-containing) plastid groups (Figure 1). By 1200 Ma, the red algae appear to have been among the first group of organisms to differentiate into multicellular forms. Cyanobacteria dominated primary production during most of the Paleoproterozoic; eukaryotic green algae became increasingly important toward the end of the Proterozoic (543 Ma) (Tappan 1980; Knoll 1989, 1992; Lipps 1993; Knoll *et al*., Chapter 8, this volume).

The now-extinct eukaryotic acritarchs were unicellular, noncolonial, organic-walled microfossils of unknown polyphyletic affinity that include the phycomata and vegetative cells of the green Prasinophyceae algae (Stover *et al*. 1996). They appeared in the fossil record by ~1700–1900 Ma (Zhang 1986; Summons *et al*. 1992) and were clearly an important component in the fossil record in the mid- to late Proterozoic. Acritarchs diversified beginning ~800–900 Ma (Knoll 1994; Knoll *et al*. 2006) during the early stages of rifting

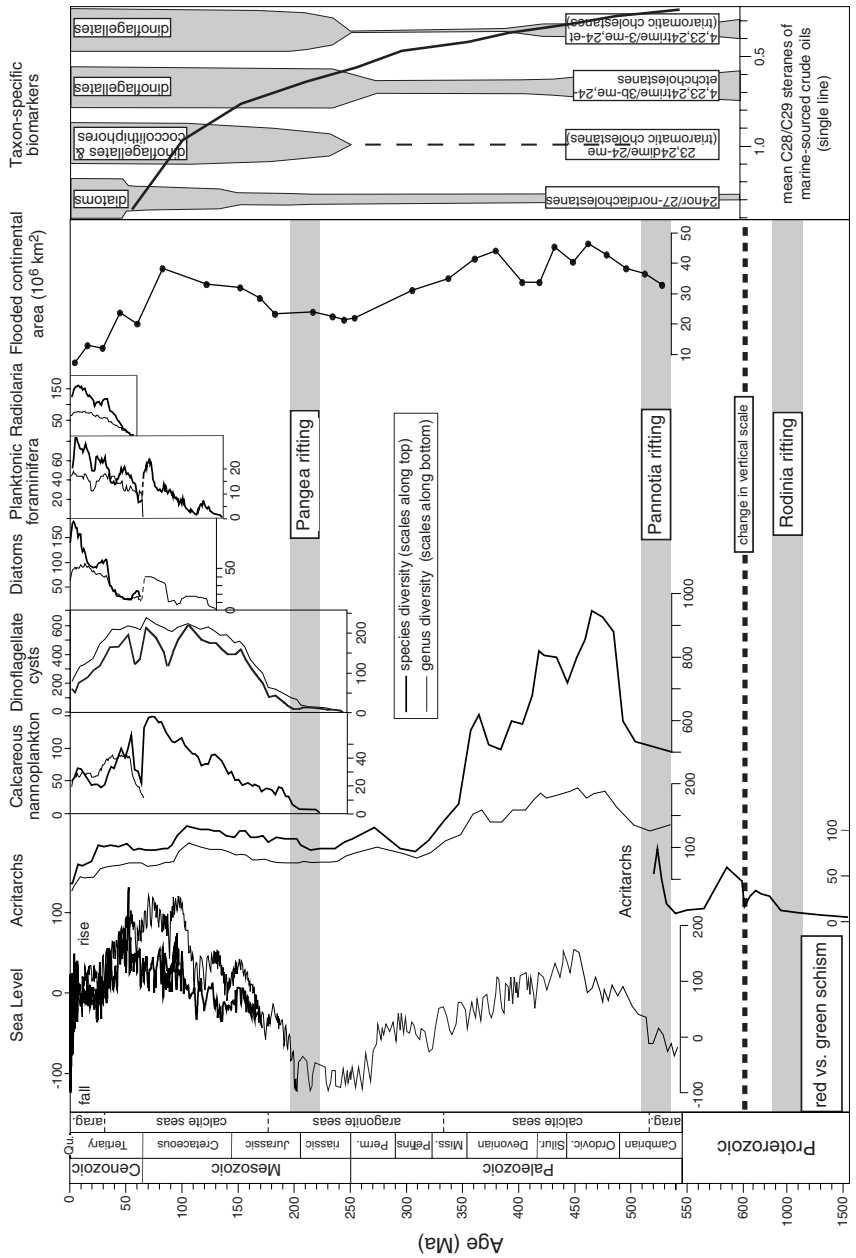

FIGURE 1. Comparison of eukaryotic phytoplankton diversity curves with zooplankton diversity curves (this study), sea-level change (Mesozoic-Cenozoic: Miller *et al*. 2005, dark line, scale at top; Haq *et al*. 1987, light line, scale at bottom; Paleozoic: Vail *et al*. 1977, light line, scale at bottom), flooded continental areas (Ronov 1994) (after Katz *et al*. 2004). Phytoplankton and zooplankton species (dark line, scale at top) and genus (light line, scale at bottom) diversities are from published studies or were compiled for this study from publicly available databases: calcareous nannofossils (species—Bown *et al*. 2004; genus—Spencer-Cervato *et al*. 1999), dinoflagellates (Stover *et al*. 1996), diatoms (Spencer-Cervato 1999), acritarchs (Proterozoic: Knoll 1994; Phanerozoic: R.A. MacRae, unpublished data), planktonic foraminifera (Spencer-Cervato 1999), and radiolaria (Spencer-Cervato 1999). All records are adjusted to the Berggren *et al*. (1995) (Cenozoic), Gradstein (Gradstein *et al*. 1995) (Mesozoic), and GSA (http://rock.geosociety.org/science/timescale/timescl.htm) (Paleozoic) time scales. Taxon-specific biomarkers (Moldowan and Jacobson 2000) and C_{28}:C_{29} sterane ratios (Grantham and Wakefield 1988) provide a record of increased biomass preservation of eukaryotic phytoplankton in the Mesozoic-Cenozoic. Episodes of supercontinent rifting are shaded.

of the supercontinent Rodinia, perhaps in response to the expansion of physical space as well as ecological niches along growing continental margins (see Figure 1). Acritarchs underwent a second expansion in concert with the early Paleozoic radiations of marine invertebrates (Knoll 1994); their diversity peaked in the mid-Paleozoic and declined rapidly in the late Devonian to early Mississippian.

B. The Rise of the Red Lineage

In the early Mesozoic, the red eukaryotic phytoplankton began to displace green eukaryotic algae in the marine realm (e.g., Falkowski *et al*. 2004b) (see Figure 1). Marine prasinophytes declined in the Jurassic, although this group of green algae is extant as a minor constituent. A period of transition to red-line–dominated primary production began in the Triassic to Early Jurassic, ultimately resulting in the dominance of coccolithophores, dinoflagellates, and diatoms in the contemporary ocean.

The first unequivocal appearance of dinoflagellates in the fossil record occurs as organic-walled relict cysts in Middle Triassic continental margin sediments (Stover *et al*. 1996). Although molecular biomarker studies indicate that dinoflagellates may have existed as far back as the Neoproterozoic (Summons and Walter 1990; Moldowan and Talyzina 1998; Knoll *et al*., Chapter 8, this volume), these biomarkers did not become prominent constituents of marine bitumens until the Triassic (Moldowan *et al*. 1996; Moldowan and Jacobson 2000), when microfossils more clearly document their expansion and radiation (Fensome *et al*. 1996; Stover *et al*. 1996) (see Figure 1).

The calcareous nannoplankton (dominated by coccolithophorids) originated in the Late Triassic and were the second group in the red lineage to radiate in the fossil record (Bown *et al*. 2004) (see Figure 1), at about the same time that molecular biomarkers of coccolithophorids became common (Moldowan and Jacobson 2000). The earliest nannoplankton have been identified in Carnian sediments from the southern Alps (Janofske 1992; Bown 1998; Bown *et al*. 2004) and Nevada (F. Tremolada, personal communication).

The diatoms were the last of the three major groups of the red lineage to emerge in the Mesozoic. The highly soluble siliceous diatom frustules may impart a preservational bias to the fossil record of diatoms. Reports of diatom frustules in Jurassic sediments (Rothpletz 1896) have proven difficult to replicate, yet molecular biological clock estimates (Medlin *et al*. 2000) and molecular biomarkers (Moldowan and Jacobson 2000) indicate that diatoms may have evolved earlier but remained minor components in the marine realm until the Cretaceous. The first unequivocal fossil record of diatoms document Early Cretaceous radiations (Harwood and Nikolaev 1995; Kooistra *et al*., Chapter 11, this volume). Early diatom morphologies were dominated by cylindrical and long-cylindrical forms that show very little variation (Gersonde and Harwood 1990; Harwood and Gersonde 1990); the morphological similarity among early diatoms suggests a common ancestor of early Mesozoic origin (Harwood and Nikolaev 1995). Late Cretaceous diatom morphologies were dominated by discoidal and biddulphioid frustules (Harwood and Nikolaev 1995). Diatoms appeared in nonmarine environments by 70 Ma (Chacon-Baca *et al*. 2002).

Regardless of the exact timing of the evolutionary origins of coccolithophores, dinoflagellates, and diatoms, fossil and biomarker data document the major expansion of all three groups in the Mesozoic (Grantham and Wakefield 1988; Harwood and Nikolaev 1995; Stover *et al*. 1996; Moldowan and Jacobson 2000; Bown *et al*. 2004) (see Figure 1). They began their evolutionary trajectories to ecological prominence when the supercontinent Pangea began to break apart and the Atlantic Ocean basin opened in the Late Triassic–Early Jurassic (~200 Ma), marking the opening phase of the current Wilson cycle (Wilson 1966; Worsley *et al*. 1986).

When Pangea was fully assembled, the larger-celled phytoplankton with high nutrient requirements most likely were concentrated along the supercontinent margins where nutrient supply was greatest, whereas the small-celled plankton (e.g., cyanobacteria) likely better competed in the large, oligotrophic Panthalassic Ocean (Finkel, Chapter 15, this volume). The balance between large- and small-celled photoplankton began to shift as Pangea started to rift in the Jurassic. Sea level rose as Pangea fragmented and the Atlantic Ocean basin widened, flooding broad continental shelves and low-lying inland areas (see Figure 1). The fragmentation of the continents and creation of a new ocean basin produced an increase in the total length of coastline where many plankton lived. Nutrients (such as phosphate) that were previously locked up in the large continental interior of Pangea were transported to newly formed shallow seas and distributed over wider shelf areas and longer continental margins; in addition, models predict that the hydrological cycle accelerated when Pangea rifted, delivering more nutrients to the oceans (Wallman 2001). These changes were profound: Greater nutrient availability coupled with expanded ecospace and ecological niches appears to have selected for the large-celled phytoplankton that lived along continental margins and contributed to their rapid radiation and evolution. Accordingly, the diversities of eukaryotic phytoplankton of the red lineage parallel sea-level rise through the Mesozoic (see Figure 1).

The Cretaceous–Tertiary boundary bolide impact caused mass extinctions (Alvarez *et al*. 1980) that are recorded in the fossil records of the calcareous nannoplankton and, to a lesser extent, the diatoms and dinoflagellates (see Figure 1). Dinoflagellates and calcareous nannoplankton recovered to near pre-extinction diversity levels by the earliest Eocene (~55 Ma), only to decline through the rest of the Cenozoic as long-term sea level fell.

In contrast to the other phytoplankton, diatom diversity has increased through the Cenozoic despite shrinking niche availability due to falling sea level. Increased bioavailability of silica may have contributed to this radiation of diatoms. Diatoms require orthosilicic acid to form extremely strong shells called frustules (Falciatore and Bowler 2000). Silica is supplied to the oceans primarily from continental weathering, a process that was accelerated by the mobilization of silica from soils by grasses because grasses contain up to 15% silica in phytoliths (micromineral deposits in cell walls). As grasses evolved, radiated, and expanded, increased transfer of silica to the oceans (primarily via fluvial erosion and, secondarily, via aeolian transport) increased the bioavailability of silica for diatom growth (Falkowski *et al*. 2004a, b). This mechanism may account for the close correlation between the evolutionary histories of grasses, terrestrial grazing animals, and diatoms.

The oldest grass phytoliths (70 Ma, Late Cretaceous) are preserved in coprolites of sauropod dinosaurs (Prasad *et al*. 2005); diatoms also became fairly common in the Late Cretaceous (Harwood and Nikolaev 1995). Although grasslands remained sparse in the Paleocene and Eocene (65–33.7 Ma), the increased abundance of phytoliths in the marine record beginning in the mid-Eocene (Retallack 2001) indicates increased delivery of bioavailable silica to the oceans (Falkowski *et al*. 2004a, b). Near the Eocene–Oligocene boundary, grasslands expanded (Retallack 2001), grazers displaced browsers (Janis and Damuth 2000), and diatoms diversified (Spencer-Cervato 1999) (see Figure 1). A second pulse of diversification occurred in the middle to late Miocene, when the further expansion of grasslands (including a shift from C_3 to C_4 grasses) (Retallack 1997, 2001) was accompanied by a second pulse of diatom diversification at the species level (Falkowski *et al*. 2004a, b). Through the Cenozoic, diatoms have been increasingly successful in outcompeting radiolaria (siliceous zooplankton) for silica (Harper and Knoll 1975; Kidder and Erwin 2001)

(see Section IV.B for discussion of Phanerozoic siliceous sedimentation).

The long-term success of diatoms in the Cenozoic may also be attributed in part to increasing latitudinal thermal gradients and decreasing deep-ocean temperatures that have contributed to greater vertical thermal stratification in the latter half of the Cenozoic (Falkowski *et al*. 2004a). These changes increased the importance of wind-driven upwelling and mesoscale eddy turbulence, which provide nutrients to the upper ocean. Sporadic nutrient influx to the euphotic zone may favor diatoms over coccolithophores and dinoflagellates, and a change in concentration and pulsing of nutrients may favor small diatoms over large diatoms. As a result, there has been a significant decrease in the average size of diatoms in the Cenozoic, with periods of change concentrated in the mid- to late Eocene and early to mid-Miocene (Finkel *et al*. 2005).

C. Biological Overprint of the Geological Carbon Cycle

There is a clear link between the history of phytoplankton evolution and the carbon cycle. In the contemporary ocean, marine phytoplankton are responsible for almost half of Earth's annual net primary production (Field *et al*. 1998) and are major contributors to export production (e.g., Falkowski and Raven 1997; Dugdale *et al*. 1998; Smetacek 1999; Laws *et al*. 2000). The efficiency of export of organic matter from the surface to the ocean interior depends on specific phytoplankton groups (Falkowski 1998; Armstrong *et al*. 2002). Although zooplankton fecal pellets (Urrere and Knauer 1981) and marine snow (Shanks and Trent 1980) can accelerate the sinking of organic matter (Smayda 1969, 1970), the direct flux of large eukaryotic phytoplankton accounts for a large fraction of the export flux. In addition, many eukaryotic phytoplankton have armor that is denser than seawater (Hamm and Smetacek, Chapter 14, this volume), predisposing them to sink. Although cyanobacteria numerically dominate the oceanic phytoplankton community today, their extremely small size (ca. 10^{-2}–$10^{2}\,\mu m^{3}$) greatly reduces their sinking rate. In contrast, eukaryotic phytoplankton, which range in size from ca. 10^{1} to more than $10^{6}\,\mu m^{3}$, have much greater potential sinking rates and also are much more likely to be incorporated into fecal pellets of macrozooplankton, which also contribute significantly to the overall export of organic matter (Roman *et al*. 2002).

On time scales of centuries, the export of organic matter from the surface to the ocean interior helps to maintain a lower partial pressure of CO_2 in the atmosphere (Volk and Hoffert 1985). However, on geological time scales, some small fraction of the exported carbon becomes incorporated into marine sediments, where it is effectively removed from the mobile carbon pools of the atmosphere and oceans (Falkowski *et al*. 2003). In addition to the size and composition of particles, the fraction of sinking material that reaches the sediments also depends on depth of the water column (Betzer *et al*. 1984; Martin *et al*. 1987). Carbon burial is most efficient on shallow continental margins (Premuzic 1980; Hedges and Keil 1995), where both export production and sedimentation rates are high (Falkowski *et al*. 1994). Hence, the area of shallow seas and length of coastlines along tectonically passive margins potentially influences the net burial of the export flux. Therefore, the taxonomic composition and cell size of phytoplankton communities that have the potential to control export flux, combined with the geographic extent of shallow seas and coastlines determined by tectonic processes, has the potential to determine the fraction of organic matter buried in marine sediments. These processes, in turn, impact the carbon cycle, the redox state of the oceans, and the long-term concentration of CO_2 in the atmosphere (Hayes and Waldbauer 2006).

III. THE PHANEROZOIC CARBON ISOTOPE RECORD

The sequestration of organic matter in marine sediments leads to changes in the isotopic composition of the mobile pools of inorganic carbon in the ocean and atmosphere. Hence, knowledge of isotopic variations in both carbonates and organic matter can be used to constrain the numerical solution to the isotopic mass balance equation (Equation 1). Let us now consider the carbon isotopic records in carbonates and organic matter throughout the Phanerozoic.

There are two major Phanerozoic carbon isotope compilations. Veizer *et al*. (1999) compiled $\delta^{13}C_{carb}$ of many fossil groups including brachiopods, belemnites, oysters, planktonic and benthic foraminiferas, and corals. Although there are some issues regarding the preservation of some of the samples in the compilation, selected data have been used extensively to infer oxygen and CO_2 concentrations over the past 550 million years (Berner 2001, 2004, 2006). Hayes *et al*. (1999) compiled published and unpublished $\delta^{13}C_{org}$ and then modified the data based on several criteria to produce a smoothed $\delta^{13}C_{org}$ curve for the past 800 million years; unfortunately, the authors have neither electronic nor paper files of their unmodified datasets (Hayes, personal communication). Hence, it is not possible to construct a high-resolution record from the low-resolution, time-averaged, modified data reported in Hayes *et al*. (1999).

In order to constrain the carbon isotopic mass balance, we developed high-resolution datasets from the Jurassic to present (Falkowski *et al*. 2005; Katz *et al*. 2005a). Because this interval spans the record of extant marine sediments, it is more accessible to isotopic analyses than older periods in Earth's history. We produced new isotopic curves from this interval for two major reasons: (1) to utilize uniform, unaltered, and suitable sample material that provide the highest quality isotopic analyses and (2) to achieve tight stratigraphic control of high-resolution datasets. Bulk sediment samples were analyzed because they best characterize the carbon outflow from the ocean/atmosphere/biosphere, and provide the average $\delta^{13}C$ of the total carbonate and organic carbon sequestered in marine sediments (Shackleton 1987; Katz *et al*. 2005a), allowing us to monitor long-term changes in the global carbon cycle through time. We specifically elected not to use carbon isotope records generated from specific organisms, which may reflect the different environments where each of those organisms lived (e.g., nearshore surface ocean versus deep-ocean bottom water), rather than the average $\delta^{13}C$ output from the system.

We analyzed samples from open ocean Atlantic Deep Sea Drilling Project (DSDP) and Ocean Drilling Program (ODP) boreholes with well-documented magnetobiostratigraphies that provide excellent age control and minimize the risk of undetected unconformities. Using open ocean locations circumvents problems that may be encountered in analyzing epicontinental sections, such as unconformities associated with sea-level changes and local overprint of geochemical signals (e.g., Smith *et al*. 2001). It was necessary, however, to use an epicontinental section for the older record because there is little to no pre-Middle Jurassic ocean floor left. We chose a single location (Mochras Borehole, Wales) that spans the entire Lower Jurassic, with well-documented lithology and biostratigraphy (Ivimey-Cook 1971; Woodland 1971).

We determined the isotopic composition of both carbonates (Shackleton and Hall 1984; Katz *et al*. 2005a) and organic matter (Falkowski *et al*. 2005) from a series of Atlantic marine sediment cores from the Lower Jurassic through the Cenozoic (Figure 2). These carbon isotope data are coeval, high-resolution (225,000-year average sampling interval) records from both carbonates and organic matter that cover the past 205 million years, providing full constraint on the carbon sinks. Correlations to shorter duration records of transient

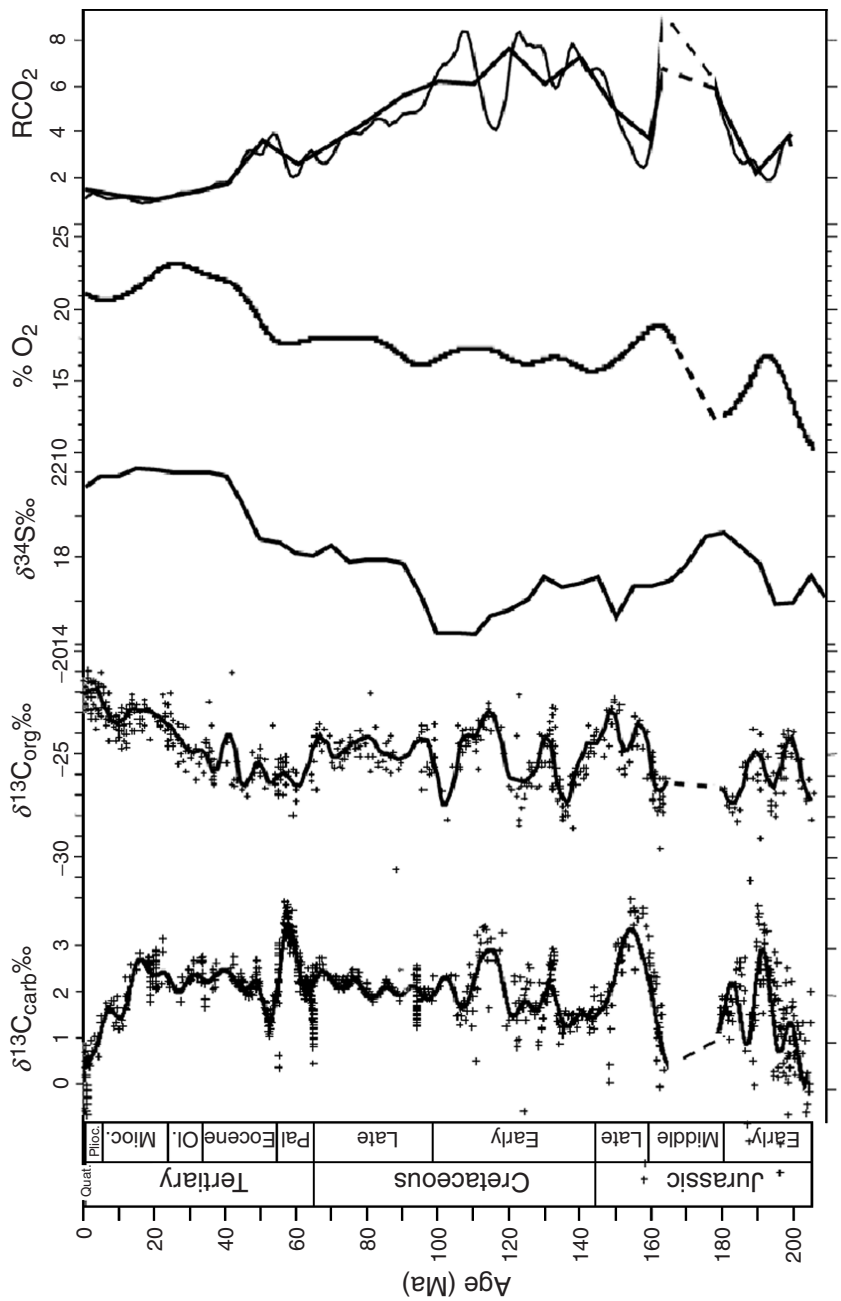

FIGURE 2. Three isotopic signatures ($\delta^{13}C_{carb}$, $\delta^{13}C_{org}$, and $\delta^{34}S_{sulf}$; Kampschulte and Strauss 2004; Falkowski *et al.* 2005; Katz *et al.* 2005a) were used to reconstruct atmospheric O_2 (Falkowski *et al.* 2005) and atmospheric CO_2 (reported as levels relative to today, RCO_2; the low-resolution record is from Katz *et al.* 2005b; the high-resolution record was produced for this study) for the Jurassic-Cenozoic. We generated RCO_2 curves using two generations of Berner's GEOCARB/GEOCARBSULF modeling series (Berner and Kothavala 2001; Berner 2006).

$\delta^{13}C$ excursions (thousand-year scale) and $\delta^{13}C$ events (3–20 million years) establish the global nature of the $\delta^{13}C_{carb}$ dataset (Katz *et al*. 2005a). The $\delta^{13}C_{carb}$ record reveals a 190 million-year increase of ~1.1‰ from the early Jurassic through the mid-Miocene and a subsequent ~2.5‰ decrease (see Figure 2). Statistical analysis of the regression of the ~1.1‰ long-term increase indicates that the slope is significantly different from zero ($P < 0.05$). The long-term increase is supported by combining Figures 2 and 3 from Hayes *et al*. (1999); when spliced together, the resulting $\delta^{13}C_{carb}$ record shows a long-term increase of ~1‰ from 200–20 Ma that was not identified. Over the same time period, statistical analysis of the $\delta^{13}C_{org}$ record also reveals a long-term secular increase of ~5‰ (Falkowski *et al*. 2005), indicating that organic matter became depleted in the light carbon isotope.

A. Jurassic to Mid-Miocene 1.1‰ $\delta^{13}C_{carb}$ Increase

The simultaneous increases in $\delta^{13}C_{carb}$ and $\delta^{13}C_{org}$ highlight a long-term increase in $\delta^{13}C$ of the mobile carbon reservoir (see Figure 2), which could have been driven by a combination of two processes: (1) an increase in the $\delta^{13}C$ of input carbon ($\delta^{13}C_{input}$) and/or (2) an increase in the fraction of organic carbon buried (f_{org}). To investigate the extent to which each of these two processes contributed to the long-term $\delta^{13}C$ increases, we ran model simulations based on a derivation of Equation 1:

$$f_{org} = \left[\left(\delta^{13}C_{input}\right) - \left(f_{carb} * \delta^{13}C_{carb}\right)\right] / \delta^{13}C_{org} \quad (2)$$

Four model runs are shown (Figure 3) that use the $\delta^{13}C_{carb}$ (Katz *et al*. 2005a) and $\delta^{13}C_{org}$ (Hayes *et al*. 1999; Falkowski *et al*. 2005) datasets to calculate the burial fractions of carbonate versus organic carbon. In the first set of model runs, $\delta^{13}C_{input}$ was allowed to vary according to parameters described in GEOCARB III (Berner and Kothavala 2001), which include various feedbacks and variables such as the influence of land plants on weathering, global temperature, paleogeography, and continental water discharge (see Berner and Kothavala 2001 for details of the model). In the second set of simulations, $\delta^{13}C_{input}$ was held constant at −5‰, based on the assumption that carbonate and organic carbon weathering from the continents averages out to this contemporary mantle carbon value (−5‰) over long time periods (e.g., Kump and Arthur 1999). The results from both of these analyses indicate that increases in $\delta^{13}C_{carb}$ and $\delta^{13}C_{org}$ require an f_{org} increase of ~0.05–0.1, regardless of whether $\delta^{13}C_{input}$ is allowed to vary (Berner and Kothavala 2001) or is held constant (Kump and Arthur 1999), and regardless of whether the high- (Falkowski *et al*. 2005) or low- (Hayes *et al*. 1999) resolution $\delta^{13}C_{org}$ dataset was used (see Figure 3). Hence, the long-term increase in the burial of organic carbon implied in the isotopic records requires greater burial efficiency (i.e., long-term sequestration) of organic matter in marine and/or terrestrial environments.

Sensitivity tests establish that neither excess burial of organic matter (marine and/or terrestrial) nor increase in $\delta^{13}C_{input}$ alone can account for the measured $\delta^{13}C$ changes (Berner and Kothavala 2001; Katz *et al*. 2005a). Rather, increases in both the extraction of ^{12}C from, and supply of ^{13}C to, the mobile carbon reservoir are required to account for the measured changes in $\delta^{13}C_{carb}$ and $\delta^{13}C_{org}$ (Falkowski *et al*. 2005; Katz *et al*. 2005a). Following this logic, we conclude that the concurrent changes in the isotopic composition of both organic and inorganic carbon pools must have occurred through (1) an increase in net burial of organic carbon in the lithosphere, which implies a net increase in the oxidation state of the atmosphere (Falkowski *et al*. 2005; Katz *et al*. 2005a), and (2) an increase in $\delta^{13}C$ of carbon introduced to the mobile carbon reservoir from volcanic outgassing and weathering of continental rocks (Caldeira 1992; Schrag 2002; Katz *et al*. 2005a).

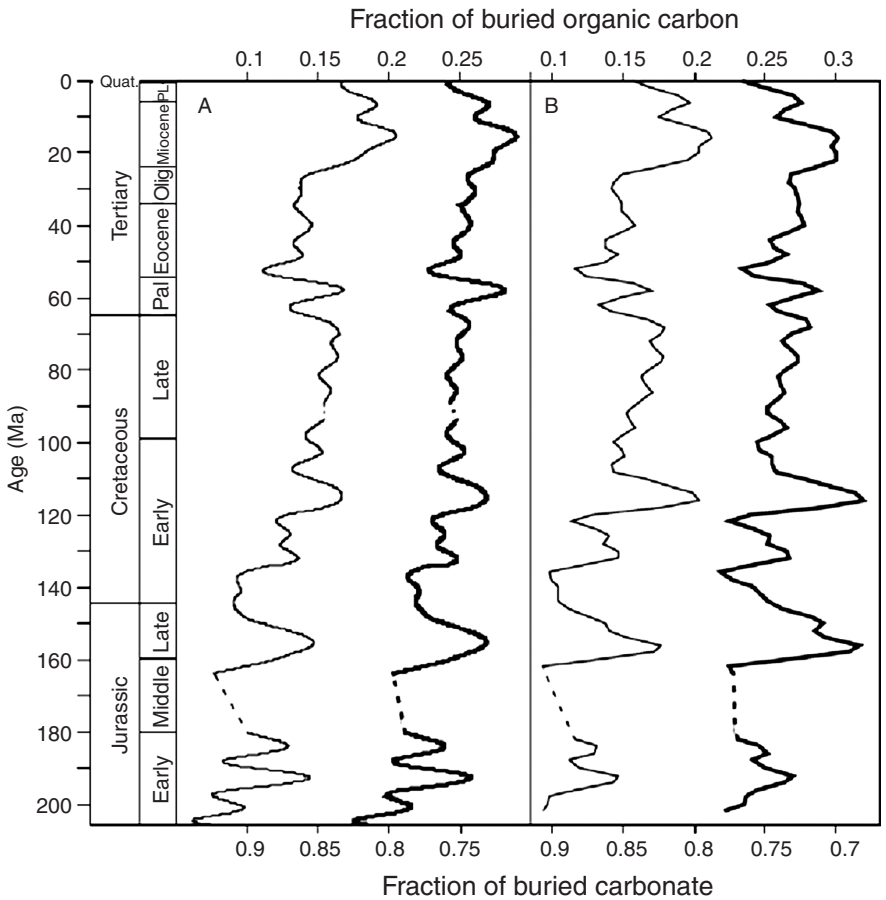

FIGURE 3. Four model simulations use the high-resolution $\delta^{13}C_{carb}$ (Katz *et al*. 2005a) and $\delta^{13}C_{org}$ (**Panel A** uses Hayes *et al*. 1999; **Panel B** uses Falkowski *et al*. 2005) datasets with two input (source) carbon scenarios (dark line: $\delta^{13}C_{input} = -5‰$; light line: variable $\delta^{13}C_{input}$ according to Berner and Kothavala [2001] parameters) to predict variations in the burial of carbonate (f_{carb}) relative to organic carbon (f_{org}) through time. Each model run shows that the measured $\delta^{13}C_{carb}$ and $\delta^{13}C_{org}$ datasets require an f_{org} increase of ~0.05–0.1, despite different datasets and input carbon parameters. This requires greater burial efficiency (i.e., long-term sequestration) of organic matter in marine and/or terrestrial environments through time.

Near the Eocene–Oligocene boundary (~33 Ma), $\delta^{13}C_{org}$ began to increase more rapidly (Hayes *et al*. 1999), whereas the rate of increase in $\delta^{13}C_{carb}$ (Shackleton and Hall 1984) remained relatively constant until ~15 Ma (see Figure 2). These records indicate that f_{org} increased during this interval to the highest level of the past 205 million years (see Figure 3), culminating in the "Monterey Carbon Excursion" in which large amounts of organic-rich, diatomaceous sediments were deposited in marginal basins (Vincent and Berger 1985).

B. 2.5‰ $\delta^{13}C_{carb}$ Decrease Since the Mid-Miocene

$\delta^{13}C_{carb}$ values have decreased by ~2.5‰ since ~15 Ma (Shackleton and Hall 1984), whereas $\delta^{13}C_{org}$ values have continued to increase (Hayes *et al*. 1999) (Figure 2). This requires an increase in ^{12}C in the mobile carbon reservoir through greater ^{12}C supply and/or less ^{12}C burial. Because Sr and Os isotopic composition varies with rock type, $^{87}Sr/^{86}Sr$ and $^{187}Os/^{186}Os$ measured in marine sediments can be used to interpret

continental weathering rates and continental source rock types. These isotopic records indicate a shift in the Neogene to continental source rocks rich in organic carbon, which may have increased the supply of ^{12}C to the oceans even though continental weathering rates may have decreased (Ravizza 1993; Derry and France-Lanord 1996; Turekian and Pegram 1997). Although an additional ~194,000 Gt of carbon from organic carbon weathering (at the expense of carbonate weathering) can account for the entire 2.5‰ $\delta^{13}C_{carb}$ decrease, the higher $\delta^{13}C_{org}$ values can in part be better attributed to the increasing importance of β-carboxylation photosynthetic pathways in marine phytoplankton and C_4 pathways in terrestrial plants in the latter part of the Cenozoic (Katz *et al*. 2005a). These pathways produce ^{13}C-enriched organic matter (i.e., higher $\delta^{13}C$ values) relative to organic matter produced through the C_3 photosynthetic pathway.

For most of the Phanerozoic, marine and terrestrial photoautotrophs used a C_3 photosynthetic pathway to fix carbon (Falkowski and Raven 1997). The long-term drawdown of CO_2 associated with greater organic carbon burial since the break-up of Pangea was a key factor that selected for new photosynthetic pathways in marine and terrestrial ecosystems. Diatoms have β-carboxylation pathways that use HCO_3^- as a substrate (Morris 1987; Reinfelder *et al*. 2000) and do not discriminate as strongly against ^{13}C (Falkowski 1997). These organisms are responsible for a disproportionate fraction of carbon export in the modern ocean (Dugdale *et al*. 1998; Smetacek 1999), especially along continental margins (Sancetta *et al*. 1991; Bienfang 1992). The rapid radiation of diatoms in the mid-Cenozoic may have resulted in marine export production that was enriched in ^{13}C (Katz *et al*. 2005a). In the mid- to late Miocene oceans, an expansion of bloom-forming diatoms (L. Burckle and R. Sombratto, personal communication) further contributed to export production of ^{13}C- enriched organic matter. In the terrestrial realm, grasslands expanded throughout most of the world in the late Miocene (6–8 Ma), accompanied by a shift in dominance from C_3 to C_4 grasses, resulting in ^{13}C-enriched terrestrial biomass (Cerling *et al*. 1997; Still *et al*. 2003). Consequently, ^{13}C-enriched terrestrial organic matter was ultimately transferred to and sequestered in the oceans (France-Lanord and Derry 1994; Hodell 1994) at the same time that ^{13}C-enriched diatoms continued to expand and export ^{13}C-enriched organic matter to the seafloor. The rise of β-carboxylation and C_4 photosynthetic pathways can account for a 1.1‰ decrease in $\delta^{13}C_{carb}$ (based on the measured $\delta^{13}C_{org}$, and assuming that $\delta^{13}C_{input}$ remained the same). The remaining ~1.4‰ decrease requires an additional ~110,000 Gt of organic carbon weathered from organic-rich shales (Katz *et al*. 2005a), as discussed previously.

IV. FEEDBACKS IN BIOGEOCHEMICAL CYCLES

Various components of global paleobiogeochemical systems can undergo complex interactions and feedbacks through time. Evidence of these interactions is recorded in geological records. Fossil evidence for phytoplankton evolutionary pulses appear to have been associated with the past three Wilson cycles. In turn, changes in continental configurations and evolutionary shifts have influenced marine sedimentation patterns and global climates. In this chapter, we have suggested there may be a causal relationship between the large-scale tectonics of the current Wilson cycle and biogeochemical cycles driven, at least in part, by changing phytoplankton community structure. Let us now take a closer look at past Wilson cycles, macroevolutionary changes, and biogeochemical cycles.

A. Phytoplankton Community Structure and the Wilson Cycle

Earlier studies suggested a correlation between evolutionary pulses in the marine realm and the Wilson cycle (e.g., Valentine

and Moores 1974; Fischer 1984; Rich *et al*. 1986; Worsley *et al*. 1986) and provided a basis for developing hypotheses about causal rather than casual linkages between these two processes (Katz *et al*. 2004). Biological diversity is maintained by isolation or fluctuations in habitat areas (MacArthur and Wilson 1967; Rosenweig 1995). The apparent correlation between phytoplankton species diversity and the Wilson cycle suggests that the break-up of supercontinents created new, unstable physical habitats for the eukaryotic phytoplankton groups that lived along continental perimeters (Katz *et al*. 2004). As the supercontinent Rodinia rifted in the Late Proterozoic, early eukaryotic acritarchs began to expand (see Figure 1). At this time, surface waters were somewhat oxic, whereas subsurface water masses were either anoxic or sulfidic (Anbar and Knoll 2002). Higher nutrient levels and better oxygenated waters in coastal regions may have favored early phytoplankton of the red lineage, whereas the phytoplankton of the green lineage outcompeted in oligotrophic open ocean surface waters that were underlain by anoxic or sulfidic deepwaters that delivered a different suite of trace elements to the surface (Whitfield 2001; Anbar and Knoll 2002; Katz *et al*. 2004).

Acritarchs diversified again in the Early Paleozoic when the supercontinent Pannotia rifted. Sea-level rise and flooded continental area associated with rifting are highly correlated with increasing diversity of Paleozoic acritarch genera and Mesozoic calcareous nannoplankton (e.g., coccolithophorids) and dinoflagellates (see Figure 1). Although flooded continental area is a small percentage of the total oceanic area suitable for phytoplankton habitat, the shallow seas appear to have contributed proportionally more to niche space because of high nutrient input, high rates of primary production, and habitat heterogeneity (Katz *et al*. 2004).

Although there is a conceptual connection between the Wilson cycle and phytoplankton diversification, more evidence is needed to establish a conclusive causal link between the tectonic cycles and evolutionary pulses. Regardless of the causal link, there also appears to be a strong connection among the current Wilson cycle, evolutionary changes in phytoplankton community structure, and long-term changes in the carbon cycle.

When Pangea was fully assembled in the Triassic, the larger-celled plankton with high nutrient requirements most likely were concentrated along the supercontinent perimeter where nutrient supplies were highest, whereas the small-celled plankton (e.g., cyanobacteria) probably better competed in the large, oligotrophic Panthalassic Ocean. As Pangea started to rift and the Atlantic Ocean basin widened in the Jurassic, sea level rose and flooded broad continental shelves and low-lying inland areas (see Figure 1). The fragmentation of the continents and creation of a new ocean basin increased the total length of coastline where many plankton lived. Nutrients (such as phosphate) that were previously locked up in the large continental interior of Pangea were transported to newly formed shallow seas and distributed over wider shelf areas and longer continental margins. Furthermore, models predict that the accelerated hydrological cycle associated with Pangea fragmentation delivered more nutrients to the oceans (Wallman 2001). These changes were profound: Greater nutrient availability coupled with expanded ecospace and ecological niches appears to have selected for the large-celled phytoplankton that lived along continental margins and contributed to their rapid radiation and evolution. This is supported by both diversity curves and biomarker studies that show increases in biomass of coccolithophores, dinoflagellates, and diatoms in the Mesozoic (see Figure 1).

In the Mesozoic, the radiation of large-celled eukaryotic marine phytoplankton (Grantham and Wakefield 1988; Moldowan and Jacobson 2000) that were efficient export producers contributed to an overall increase in export production through time (Bambach 1993; Falkowski *et al*. 2003; Katz

et al. 2005a). Much of the export production is concentrated along continental margins today (Walsh 1988; Laws *et al*. 2000), where up to 90% of organic carbon burial occurs (Hedges and Keil 1995). In the Mesozoic, substantial amounts of organic carbon were sequestered on the newly formed passive continental margins of the Atlantic and on flooded continental interiors (Claypool *et al*. 1977; Arthur *et al*. 1984; Jenkyns and Clayton 1997; Bralower 1999) as Pangea broke apart. This in effect has provided a long-term storehouse of ^{12}C-enriched organic matter during the current Wilson cycle (Katz *et al*. 2005a). Global sediment budgets indicate that an order of magnitude more sediment is deposited in ocean basins than is subducted (Rea and Ruff 1996) and that the long-term marine sedimentary system can be at steady state only over a complete Wilson cycle (Mackenzie and Pigott 1981; Worsley *et al*. 1986; Rea and Ruff 1996); however, sedimentary accretion on cratons has the potential to keep the system out of balance even over several Wilson cycles (e.g., Katz *et al*. 2005a; Hayes and Waldbauer 2006), as discussed previously.

These results support the hypothesis that the Phanerozoic Wilson cycles drove the greenhouse–icehouse cycles (Fischer 1984), in what is essentially a carbon redox-mediated climate system (Worsley and Nance 1989). In this scenario, volcanic CO_2 outgassing during continental fragmentation created greenhouse climates, and atmospheric CO_2 drawdown due to weathering processes eventually switched the planet to an icehouse mode. Icehouse intervals with major glaciations tend to be associated with times of either supercontinent assembly or maximum continent dispersal (Worsley and Nance 1989). There may well be a significant biological component that contributes to the climate switch (Katz *et al*. 2005a). This important additional biological loop connects changes in phytoplankton community structure that contributed to greater efficiency of organic carbon burial beginning in the Early Jurassic to the excess carbon burial that drove the net oxidation of Earth's surface reservoirs and atmospheric CO_2 drawdown during the opening phase of the current Wilson cycle. This ultimately contributed to the climate change from the greenhouse conditions of the Mesozoic to the icehouse conditions that characterize the latter half of the Cenozoic (Katz *et al*. 2005a).

B. Biological Impact on Global Sedimentation Patterns

The distribution of carbonate deposition in the oceans over hundreds of millions of years has been determined by a complex set of parameters. Continental distributions coupled with global sea level determine the area of flooded tropical shelves, which in turn factors into the amount of shallow-water carbonate accumulation (Wilkinson and Algeo 1989; Walker *et al*. 2002). The poleward migration of continents over the past 540 million years has decreased carbonate accumulation, as has falling sea level through the Cenozoic, by decreasing the areal extent of shallow tropical seas. As tropical carbonate deposition declined, the carbonate saturation of the oceans rose (Wilkinson and Algeo 1989; Walker *et al*. 2002). A positive feedback loop may ultimately have favored the expansion of open ocean calcifying phytoplankton and zooplankton: as discussed previously, the expansion of the larger-celled eukaryotic phytoplankton of the red-plastid lineage, coupled with the opening of the Atlantic Ocean basin and global sea-level rise, resulted in greater organic carbon burial beginning in the Early Jurassic as the supercontinent Pangea rifted. Excess organic carbon burial drove the drawdown of atmospheric CO_2. Declining pCO_2 and pH, combined with rising carbonate saturation, may have facilitated the rise of coccolithophores and planktonic foraminifera; expansion of these two groups close the loop by further contributing to export production and declining pCO_2.

The rise of coccolithophores beginning in the early Mesozoic may also have been favored by ocean chemistry associated with the Wilson cycle. As seawater cycles through mid-ocean ridges, calcium is added and magnesium is removed. Total ridge length and seafloor spreading rates can alter Mg:Ca ratios in seawater. High Mg:Ca ratios tend to occur during times of supercontinent assembly when ridge length is shortest, characterized by deposition of aragonite and high-magnesium calcite (called "aragonite seas") (see Figure 1). In contrast, low magnesium-calcite deposition tends to characterize times of continental breakup (called "calcite seas") (Sandberg 1975; Hardie 1996). Low Mg:Ca and high Ca^{+2} concentration in seawater favors calcification in several groups of marine organisms, including coccolithophores; hence, there is a correspondence between these organisms and "calcite sea" intervals (Stanley and Hardie 1998), including the expansion of coccolithophores in the Mesozoic calcite seas (see Figure 1). This correlation further links the expansion of coccolithophores to the opening phase of the current Wilson cycle, organic carbon burial increase, and declining pCO_2 and pH.

The expansion of open-ocean calcifiers (see Figure 1) altered global carbonate depositional patterns. Prior to the Mesozoic, most marine calcifying organisms lived in shallow coastal and shelf regions; as a result, carbonate deposition was concentrated in these areas, whereas deposition of pelagic carbonates was minimal. As two groups of carbonate-secreting plankton expanded in the Mesozoic oceans—coccolithophores with their calcitic-plated armor (see de Vargas *et al*., Chapter 12, this volume), and planktonic foraminifera with their carbonate tests (e.g., Tappan and Loeblich 1988)—the loci of marine carbonate deposition gradually expanded from shallow shelf areas to the deeper ocean (Sibley and Vogel 1976; Southam and Hay 1981) and the carbonate compensation depth (CCD) deepened (e.g., van Andel 1975; Wilkinson and Algeo 1989). Pelagic carbonate sedimentation has come to dominate as sea level and shelf area have declined since the Late Cretaceous, tropical shelf area has decreased as continents moved poleward, and the pelagic carbonate reservoir has increased at the expense of the shallow-water carbonate reservoir since the Mesozoic (Wilkinson and Algeo 1989).

Similarly, evolutionary trends in biosiliceous marine organisms have affected silica deposition through time (Maliva *et al*. 1989; Kidder and Erwin 2001). Inorganic precipitation and microbial activity in shallow seas were responsible for silica deposition in the Late Proterozoic and Cambrian. In the Paleozoic and much of the Mesozoic, siliceous sponges contributed most to shelf siliceous deposits (Racki 1999), whereas radiolaria were responsible for deep-ocean silica deposition (Casey 1993; Kidder and Erwin 2001). With the rise of diatoms in the Cretaceous, siliceous sponges largely vacated continental shelves and populated the deeper slope regions (Maldonado *et al*. 1999). Diatoms have outcompeted radiolaria for silica through the Cenozoic (Harper and Knoll 1975) and control silica removal from the oceans today (Treguer *et al*. 1995). As diatoms expanded in the Cenozoic oceans, radiolarian test weight declined and tests underwent structural changes to adapt to declining silica availability (Harper and Knoll 1975).

C. Effects of Carbon Burial on Atmospheric Gases

During the current Wilson cycle, the long-term increase in $\delta^{13}C$ of the mobile carbon reservoir resulted from biological and tectonic processes that acted in concert to increase the efficiency of organic carbon burial, driving the 190 million-year–long depletion of ^{12}C from the ocean-atmosphere system since the Early Jurassic. As discussed previously, this was most likely the result of increases in both f_{org} and $\delta^{13}C_{input}$, which supplied more ^{13}C to and extracted more ^{12}C from the mobile carbon reservoir

during the opening phase of the current Wilson cycle (Falkowski *et al*. 2005; Katz *et al*. 2005a). Because the ultimate source of the buried organic matter was oxygenic photosynthesis, the increase in organic carbon burial should have acted to draw down atmospheric CO_2 levels, while enriching the atmosphere with O_2.

1. *Atmospheric CO_2*

In the contemporary ocean, diatoms are responsible for ~60% of the sinking flux of particulate organic carbon (POC) (Smetacek 1999; Kooistra *et al*., Chapter 11, this volume), whereas coccolithophores are responsible for up to 80% of the particulate inorganic carbon (PIC) flux, primarily in the form of calcite (de Vargas *et al*., Chapter 12, this volume). Precipitation of calcite produces CO_2 that can be released to the atmosphere (Berner *et al*. 1983). Hence, diatoms and coccolithophores potentially can biologically modify Earth's carbon cycle, and specifically, atmospheric and surface ocean CO_2 inventories. This suggests that biological processes can modify the slow, abiotic carbon cycle, an idea that can be explored by modeling CO_2 inventories through time.

The history of Phanerozoic atmospheric CO_2, reported as ratios (R) relative to contemporary levels (RCO_2), has been reconstructed using models based on carbon isotope records and from proxy CO_2 records, including plant stomatal index, boron isotopes, planktonic foraminiferal carbon isotope, and paleosol carbon isotopes (see Royer *et al*. 2004) for summary). In general, reconstructions based on modeled RCO_2 are consistent with proxy CO_2 records. Early Paleozoic high RCO_2 fell during the Devonian land plant explosion and continued to decline to low levels during the Permo-Carboniferous, which was characterized by the longest glacial period during the Phanerozoic. RCO_2 increased beginning in the Triassic, reaching relatively high levels in the Jurassic and Early Cretaceous, and then declined through the Late Cretaceous and Cenozoic.

Published RCO_2 reconstructions that use models based on carbon isotope records have been done in 10 million year time averages (Berner and Kothavala 2001; Berner 2006), providing long-term trends in RCO_2 that do not capture the detailed changes in the global carbon cycle that are indicated by our higher resolution isotopic records. Using our high-resolution $\delta^{13}C_{carb}$ and $\delta^{13}C_{org}$ records, we modeled the short-term (1 million year) variations superimposed on the long-term RCO_2 trends in the Jurassic-Cenozoic. Our model uses the $\delta^{13}C_{carb}$ and $\delta^{13}C_{org}$ data (Falkowski *et al*. 2005; Katz *et al*. 2005a) to parameterize the GEOCARB III (Berner and Kothavala 2001) and GEOCARBSULF (Berner 2006) models of the global carbon cycle (see Figure 2). The GEOCARB models use isotope mass balance constraints to describe the long-term geochemical carbon cycle by describing the transfer of carbon between sediment/rock reservoirs and the ocean/atmosphere system. The fundamental processes are drawdown of CO_2 from the atmosphere during weathering of silicate rocks and subsequent carbonate precipitation in the ocean, breakdown of carbonate minerals via metamorphism, and the burial, weathering, and thermal breakdown of organic carbon (Berner 1991). The GEOCARB models take into account many feedbacks in the carbon system, such as the dependence of temperature and runoff on atmospheric CO_2 levels, the effects of large vascular land plants on calcium–magnesium silicate weathering, the effects of changing paleogeography on land temperatures and weathering, and the enhancement of weathering by gymnosperms versus angiosperms (Berner and Kothavala 2001).

We show two RCO_2 curves using our data in two generations of Berner's GEOCARB modeling series (Berner and Kothavala 2001; Berner 2006) (see Figure 2); both curves are roughly within the high and low RCO_2 ranges given by GEOCARB III. The lower resolution curve (Katz *et al*. 2005a) uses GEOCARBSULF (Berner 2006) in

10 million-year averages, with peak RCO_2 in the Jurassic-Early Cretaceous and decline through the Late Cretaceous-Cenozoic. Our higher resolution RCO_2 curve shows changes of up to ~50% over several ~10 million-year intervals in the Late Jurassic and Early Cretaceous; these CO_2 fluctuations are consistent with lower resolution proxy records. Short-term CO_2 fluctuations of the same magnitude have been recorded during glacial–interglacial cycles, when CO_2 ranged from 180 to 280 ppm (~50% variability) on the 100 thousand-year scale. Hence, our high-resolution RCO_2 reconstruction is consistent with published model and proxy records but provides much more temporal detail. The ~10 million-year fluctuations can be attributed to changes in the biological processes that are responsible for export production and/or the geological processes that are responsible for sediment preservation. Our results suggest that the long-term decline in RCO_2 is in part the result of the long-term increase in organic carbon sequestration, that is, CO_2 drawdown has been mediated by biological processes.

2. *Atmospheric O_2*

The carbon, sulfur, and iron cycles together are the dominant controls on the redox conditions that determine atmospheric oxygen levels through the biological processes of oxygenic photosynthesis and bacterial sulfate reduction, coupled with the geological processes that are responsible for organic carbon and pyrite sedimentation and iron oxidation (Hayes and Waldbauer 2006). The iron cycle is a small, yet important, component that contributes to average redox conditions and pO_2, but its geologic history cannot be readily reconstructed through direct measurements (Hayes and Waldbauer 2006). Therefore, the carbon and sulfur cycles are perhaps the most important of the biogeochemical cycles that can be directly measured and used to reconstruct the history of O_2 using the stable isotopic records of these elements. Three isotopic signatures ($\delta^{13}C_{carb}$, $\delta^{13}C_{org}$, and $\delta^{34}S_{sulf}$; Kampschulte and Strauss 2004; Falkowski *et al*. 2005; Katz *et al*. 2005a) were used to reconstruct atmospheric O_2 over the past 205 million years (Falkowski *et al*. 2005) by hindcasting from the present value of 21% using the isotope mass balance model of Berner and colleagues (Berner *et al*. 2000) (see Figure 2). These results indicate that atmospheric O_2 increased throughout the Mesozoic from a low in the Triassic to ~18% of the total atmospheric volume by the Late Cretaceous. Levels may have reached as high as 23% O_2 in the Eocene, followed by a small decline over the last ~10 million years. Contemporary O_2 levels were reached by 50 Ma.

Except for a few points near 200 Ma and 180 Ma, the results suggest there was sufficient oxygen throughout the Mesozoic to allow fires to burn (Chaloner 1989). Although several previous models (Berner and Canfield 1989; Berner *et al*. 2000; Hansen and Wallman 2003; Bergman *et al*. 2004) predict O_2 greater than 21% in the Cretaceous, they are based on very different sets of assumptions with predicted temporal evolution of atmospheric O_2 that are qualitatively quite different. Of these models, only one (Berner *et al*. 2000) uses isotopic mass balance and agrees with the predicted long-term increase of O_2 during the past 205 million years (Falkowski *et al*. 2005). The abundance of different rock types that reflect redox-sensitive mineral distributions (Tappan 1974; Berner and Canfield 1989) supports an increase in oxygen over this time. In contrast, the models by Hansen and Wallmann (2003) and Bergman *et al*. (2004) do not show this rise, do not use isotopic records to numerically constrain their predictions, and rely on many more assumptions than models based on isotopic mass balance.

3. *The Evolution of Placental Mammals*

The fairly rapid decline in oxygen at the end-Permian through Early Triassic may have been a major factor in the extinction of terrestrial

animals (mostly reptiles) (Huey and Ward 2005). In contrast, the rise of oxygen over the ensuing 150 million years almost certainly contributed to evolution of large animals (Figure 4). Animals with relatively high oxygen demands evolved by the Late Triassic, such as small mammals and theropod dinosaurs (the group that includes living birds) (Carroll 1988; Asher *et al*. 2005). The metabolic demands of birds and mammals are three- to sixfold higher per unit biomass than those of reptiles (Else and Hulbert 1981). In addition, placental reproduction requires relatively high ambient oxygen concentrations because of the inefficiency of gas transport through the placenta (Mortola 2001; Andrews 2002). We note that placental evolution is not unique to mammals; it is found in 54 species of extant reptiles (Shine 2005). However, the overall metabolic demands of these placental reptiles are four- to sixfold lower per unit biomass than that of mammals. Moreover, mammal fetuses have relatively high oxygen demands, which scale directly with body size (Schmidt-Nielson 1970). Few extant mammals reproduce above elevations of ca. 4500 m, corresponding to atmospheric oxygen levels in the Early Jurassic (Falkowski *et al*. 2005; Huey and Ward 2005). Ultimately, there must be sufficient atmospheric O_2 to meet both the mammalian mother's and fetus' requirements.

Although the reproductive strategies of the earliest mammals are not known with certainty, both fossil records and molecular clock models suggest that the evolution and superordinal diversification of placental mammals occurred between 65 and 100 Ma (Murphy *et al*. 2001; Springer *et al*. 2003; Asher *et al*. 2005). This radiation corresponds to a period of relatively high and stable oxygen levels in the atmosphere (see Figure 4). All modern placental mammal orders appear in the fossil record by the Eocene, corresponding to a relatively sharp increase in atmospheric oxygen levels (Falkowski *et al*. 2005).

Atmospheric oxygen may also have been a factor in determining evolutionary trends in mammal size (see Figure 4). Being homeotherms, mammals have extremely high metabolic demands. These demands require not only high caloric intake relative to poikilotherms but also high rates of oxygen supply. Oxygen is delivered to tissue via arterial networks, culminating in capillaries that serve as the actual point of diffusion of gases to tissues. Muscles are among the tissues with the highest oxygen demand. In mammals, the density of capillaries per unit muscle scales to the power of 0.87 (Weibel and Hoppeler 2005). Hence, the larger the animal, the lower the capillary density per unit muscle tissue; large mammals require high ambient O_2 levels to obtain maximal metabolic rates. The Cretaceous/Tertiary mass extinction at 65 Ma provided the ecological opportunity for an increase in small- to medium-sized mammals in the first few million years following the event (Alroy 1999). However, the increase in average mammalian body size was significantly smaller than that of Eocene placental mammals (see Figure 4). In fact, it has long been recognized that the lack of a herbivorous mammalian megafauna for the entire duration of the Paleocene is one of the more interesting and peculiar lags in the postextinction recovery phase (Wing *et al*. 1992). A second increase in mean body mass occurred in the early through middle Eocene (50–40 Ma) (Alroy 1999), followed by additional (but less dramatic) size increases through the Miocene.

Hence, a secular increase in atmospheric oxygen over the past 205 million years broadly corresponds with three main aspects of vertebrate evolution—endothermy, placentation, and size (Falkowski *et al*. 2005). Particularly notable are high stable O_2 levels during the time of placental mammal origins and diversification, along with a close correspondence between marked increases in both atmospheric oxygen levels and mammalian body size during the early to middle Eocene. Although increases in mammalian body size, morphological disparity, and inferred ecological heterogeneity during this interval may have been influenced as well by

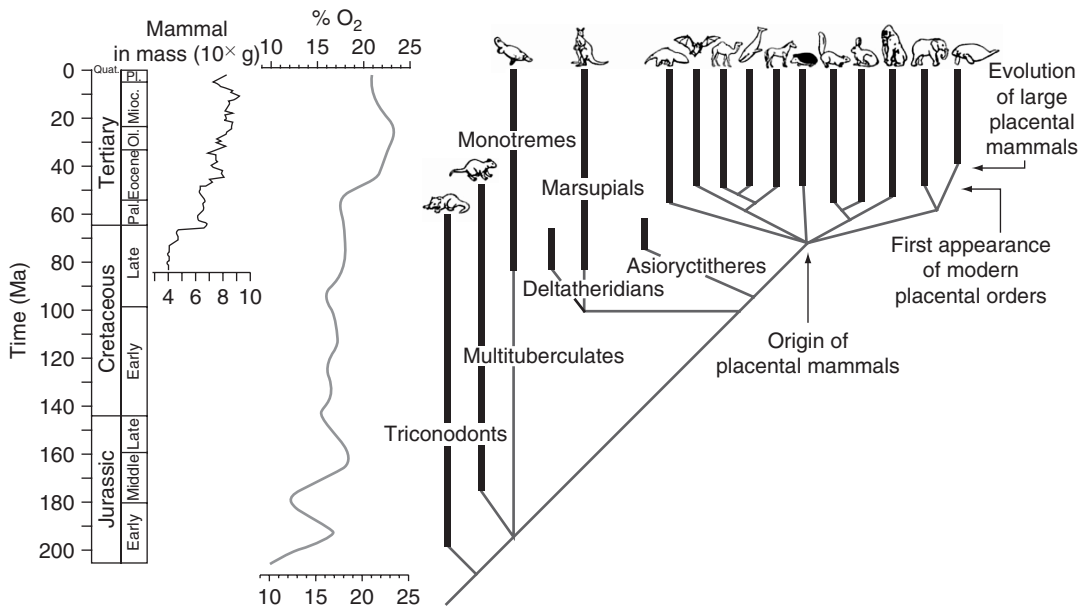

FIGURE 4. Mammal evolutionary events based on fossil, morphological (Murphy *et al*. 2001), and molecular (Murphy *et al*. 2001; Springer *et al*. 2003) evidence compared with oxygen concentrations in Earth's atmosphere modeled over the past 205 million years using carbon and sulfur isotope datasets; O_2 levels approximately doubled over this time from 10% to 21%, punctuated by rapid increases in the Early Jurassic and from the Eocene to the present. Changes in average mammalian body mass is taken from Alroy (1999). Vertical black bars represent known fossil ranges; dashed lines represent inferred phylogenetic branching. Only some of the ordinal-level placental mammals are shown. Reproduced from Falkowski *et al*. (2005). (See color plate.)

other environmental factors, the correlation between evolutionary changes in mammalian body size and increased atmospheric O_2 has a physiological basis related to placental mammal reproduction (Wing *et al*. 1992).

V. CONCLUDING REMARKS

Geological and biological processes acted in concert to modify atmospheric and seawater chemistry through time: Tectonic outgassing and erosional processes are the primary suppliers of most major elements in geochemical cycles; biologically mediated redox processes alter mobile elemental reservoirs before geological processes sequester (remove) elements from these mobile reservoirs. This biological overprint of geological processes forms complex feedback loops in biogeochemical cycles that are recorded in geochemical proxy records; these proxies, studied in conjunction with numerical models, provide a window on paleobiogeochemical interactions that form the network of Earth's system.

Carbon isotope records provide critical information that can be used to reconstruct changes in redox conditions and biological processes that affected past atmospheric and seawater chemistry. We use carbon isotope records of carbonates and organic matter, in conjunction with sulfur isotopes of sulfates, in model simulations to reconstruct carbon burial, pCO_2, and pO_2. These model results indicate that organic carbon burial and pO_2 have increased since the Early Jurassic, whereas pCO_2 has decreased since the Early Cretaceous.

We attribute these secular changes in the carbon cycle to the interplay between geological and biological processes: The evolution and expansion of the larger-celled eukaryotic phytoplankton of the red-plastid

lineage acted to increase export production, whereas continental margin ecospace and sediment storage capacity increased with the opening of the Atlantic Ocean basin and global sea-level rise as the supercontinent Pangea rifted. The resulting excess organic carbon burial increased the oxidation state of Earth's surface reservoirs while drawing down atmospheric CO_2, which in turn acted as a strong selective agent in both marine and terrestrial primary producers, resulting in the rise in C_4 and β-carboxylation photosynthetic pathways in the latter part of the Cenozoic. At the same time, atmospheric O_2 levels approximately doubled. Our analysis suggests that the rise of oxygen may have been a key factor in the evolution, radiation, and subsequent increase in the average size of placental mammals during the Cenozoic.

Acknowledgments

This study was supported by NSF OCE 0084032 Biocomplexity: The Evolution and the Radiation of Eucarytoic Phytoplankton Taxa (EREUPT). This research used samples provided by the Ocean Drilling Program (ODP), which is sponsored by the U.S. National Science Foundation (NSF) and participating countries under management of Joint Oceanographic Institutions (JOI), Inc. We thank A.H. Knoll and R.A. Berner for discussions.

References

Alroy, J. (1999). The fossil record of North American mammals: evidence for a Paleocene evolutionary radiation. *Syst. Biol*. **48:** 107–118.

Alvarez, L.W., Alvarez, W., Asaro, F., and Michel, H.V. (1980). Extraterrestrial cause for the Cretaceous-Tertiary extinction. *Science* **208:** 1095–1108.

Anbar, A.D., and Knoll, A.H. (2002). Proterozoic ocean chemistry and evolution: a bioinorganic bridge? *Science* **297:** 1137–1142.

Andrews, R. (2002). Low oxygen: a constraint on the evolution of viviparity in reptiles. *Physiol. Biochem. Zool*. **75:** 145–154.

Armstrong, R.A., Lee, C., Hedges, J.I., Honjo, S., and Wakeham, S.G. (2002). A new, mechanistic model for organic carbon fluxes in the ocean, based on the quantitative association of POC with ballast minerals. *Deep Sea Res. II* **49:** 219–236.

Arthur, M.A., Dean, W.E., and Stow, D.A.V. (1984). Models for the deposition of Mesozoic-Cenozoic fine-grained organic-C rich sediment in the deep sea. *Fine-Grained Sediments: Deep-Water Processes and Facies*. D.A.V. Stow and D.J.W. Piper, eds. Great Britain, Geological Society of London Special Publication, pp. 527–559.

Asher, R.J., Meng, J., Wible, J.R., McKenna, M.C., Rougier, G.W., Dashzeveg, D., and Novacek, M.J. (2005). Stem lagomorpha and the antiquity of glires. *Science* **307:** 1091–1094.

Bambach, R.K. (1993). Seafood through time: changes in biomass, energetics, and productivity in the marine ecosystem. *Paleobiology* **19:** 372–397.

Berggren, W.A., Kent, D.V., Swisher, C.C., and Aubry, M.-P. (1995). A revised Cenozoic geochronology and chronostratigraphy. *Geochronology, Time Scales and Global Stratigraphic Correlations: A Unified Temporal Framework for an Historical Geology*. W. A. Berggren, D. V. Kent, and J. Hardenbol, eds. Tulsa OK, SEPM (Society for Sedimentary Geology), pp. 129–212.

Bergman, N.M., Lenton, T.M., and Watson, A.J. (2004). COPSE: A new model of biogeochemical cycling over Phanerozoic time. *Am. J. Sci*. **304:** 397–437.

Berner, R.A. (1991). A model for atmospheric CO_2 over Phanerozoic time. *Am. J. Sci*. **291:** 339–376.

Berner, R.A. (2001). Modeling atmospheric O_2 over Phanerozoic time. *Geochim. Cosmochim. Acta* **65:** 685–694.

Berner, R.A. (2004). *The Phanerozoic Carbon Cycle: CO_2 and O2*. Oxford University Press.

Berner, R.A. (2006). GEOCARBSULF: a combined model for Phanerozoic atmospheric O_2 and CO_2. *Geochim. Cosmochim. Acta* **70:** 5653–5664.

Berner, R., and Canfield, D. (1989). A model for atmospheric oxygen over Phanerozoic time. *Am. J. Sci*. **289:** 333–361.

Berner, R.A., and Kothavala, Z. (2001). GEOCARB III: a revised model of atmospheric CO_2 over Phanerozoic time. *Am. J. Sci*. **301:** 182–204.

Berner, R.A., Lasaga, A., and Garrels, R. (1983). The carbonate-silicate geochemical cycle and its effect of atmospheric carbon dioxide over the past 100 million years. *Am. J. Sci*. **283:** 641–683.

Berner, R.A., Petsch, S.T., Lake, J.A., Beerling, D.J., Popp, B.N., Lane, R.S., Laws, E.A., Westley, M.B., Cassar, N., Woodard, F.I., and Quick, W.P. (2000). Isotope fractionation and atmospheric oxygen: implications for Phanerozoic O_2 evolution. *Science* **287:** 1630–1633.

Betzer, P.R., Showers, W.J., Laws, E.A., Ditullio, G.R., and Kroopnick, P.M. (1984). Primary productivity and particle fluxes on a transect of the equator at 153 degrees West in the Pacific Ocean. *Deep Sea Res*. **31:** 1–12.

Bienfang, P.K. (1992). The role of coastal high latitude ecosystems in global export production. *Primary Productivity and Biogeochemical Cycles in the Sea*. P.G. Falkowski and A. Woodhead, eds. New York, Plenum Press, pp. 285–297.

Bown, P.R. (1998). *Calcareous Nannofossil Biostratigraphy*. London, Kluwer Academic Publishers.

Bown, P.R., Lees, J.A., and Young, J. R. (2004). Calcareous nannoplankton diversity and evolution through time. *Coccolithophores: From Molecular Processes to Global Impact*. H. Thierstein, and J. R. Young, eds. Berlin, Springer-Verlag, pp. 481–507.

Bralower, T.J. (1999). The record of global change in mid-Cretaceous (Barremian-Albian) sections from the Sierra Madre, northeast Mexico. *J. Foraminiferal Res.* **29:** 418–437.

Brocks, J.J., Logan, G.A., Buick, R., and Summons, R.E. (1999). Archean molecular fossils and the early rise of eukaryotes. *Science* **285:** 1033–1036.

Broecker, W.S., and Peng, T.-H. (1982). *Tracers in the Sea*. Palisades NY, LDEO of Columbia University.

Caldeira, K. (1992). Enhanced Cenozoic chemical weathering and the subduction of pelagic carbonate. *Nature* **357:** 578–581.

Carroll, R.L. (1988). *Vertebrate Paleontology and Evolution*. New York, Freeman.

Casey, R.E. (1993). Radiolaria. *Fossil Prokaryotes and Protists*. J.H. Lipps, ed. Boston, Blackwell Scientific, pp. 249–284.

Cerling, T.E., Harris, J.M., MacFadden, B.J., Leakey, M.G., Quade, J., Eisenmann, V., and Ehleringer, J.R. (1997). Global vegetation change through the Miocene/Pliocene boundary. *Nature* **389:** 153–158.

Chacon-Baca, E., Beraldi-Campesi, H., Cevallos-Ferriz, S. R. S., Knoll, A. H., and Golubic, S. (2002). 70 Ma nonmarine diatoms from northern Mexico. *Geology* **30**:279–281.

Chaloner, W. (1989). Fossil charcoal as an indicator of palaeoatmospheric oxygen level. *J. Geol. Soc.* **146:** 171–174.

Claypool, G.E., Lubeck, C.M., Bayeinger, J.P., and Ging, T.G. (1977). Organic geochemistry. *Geological Studies on the COST No. B-2 Well, U.S. Mid-Atlantic Outer Continental Shelf Area*. P.A. Scholle, ed. U.S.G.S. Circular, pp. 46–59.

Derry, L.A., and France-Lanord, C. (1996). Neogene Himalayan weathering history and river $^{87}Sr/^{86}Sr$: impact on the marine Sr record. *Ear. Planet. Sci. Lett.* **142:** 59–74.

de Vargas, C. Probert, I., Aubry, M.P., and Young, J. (2007). Origin and evolution of coccolithophores: from coastal hunters to oceanic farmers. *Evolution of Primary Producers in the Sea*. P.G. Falkowski and A.H. Knoll, eds. Boston, Elsevier, pp. 251–285.

Drake, M.J., and Righter, K. (2002). Determining the composition of the Earth. *Nature* **416:** 39–44.

Dugdale, R., and Wilkerson, F. (1998). Silicate regulation of new production in the equatorial Pacific upwelling. *Nature* **391:** 270–273.

Else, P., and Hulbert, A. (1981). Comparison of the "mammal machine" and the "reptile machine": energy production. *Am. J. Physiol. Regul. Integr. Comp. Physiol.* **240:** 3–9.

Falciatore, A., and Bowler, C. (2000). Revealing the molecular secrets of marine diatoms. *Ann. Rev. Plant Biol.* **53:** 109–130.

Falkowski, P.G. (1997). Photosynthesis: the paradox of carbon dioxide efflux. *Curr. Biol.* **7:** R637–R639.

Falkowski, P.G. (1998). Biogeochemical controls and feedbacks on ocean primary productivity. *Science* **281:** 200–206.

Falkowski, P.G. (2001). Biogeochemical cycles. *Encyclopedia of Biodiversity.* S.A. Levin, ed. San Diego, Academic Press, pp. 437–453.

Falkowski, P.G., Biscaye, P.E., and Sancetta, C. (1994). The lateral flux of biogenetic particles from the eastern North American continental margin to the North Atlantic Ocean. *Cont. Shelf Res.* **41:** 583–601.

Falkowski, P.G., Katz, M.E., Knoll, A.H., Quigg, A., Raven, J.A., Schofield, O., and Taylor, M. (2004b). The evolutionary history of eukaryotic phytoplankton. *Science* **305:** 354–360.

Falkowski, P.G., Katz, M.E., Milligan, A., Fennel, K., Cramer, B.S., Aubry M.P., Berner, K.A., Novacek, M., and Zupole, W.M. (2005). The rise of oxygen over the past 205 million years and the evolution of large placental mammals. *Science* **309:** 2202–2204.

Falkowski, P., Laws, E.A., Barbar, R.T., and Murray, J.W. (2003). Phytoplankton and their role in primary, new and export production. M.J.R. Fasham, ed. *Ocean Biogeochemistry. The Role of the Ocean Carbon Cycle in Global Change.* Berlin, Springer-Verlag, pp. 99–121.

Falkowski, P.G., and Raven, J. A. (1997). *Aquatic Photosynthesis*. Malden, MA, Blackwell Science.

Falkowski, P.G., Schofield, O., Katz, M.E., van de Schootbrugge, B., and Knoll, A. (2004a). Color wars: why is the land green and the ocean red? *Coccolithophores: From Molecular Processes to Global Impact*. Berlin, H. Thierstein, and J.R. Young, eds. Springer-Verlag, pp. 429–453.

Fensome, R.A., MacRae, R.A., Moldowan, J.M., Taylor, F.J.R., and Williams, G.L. (1996). The early Mesozoic radiation of dinoflagellates. *Paleobiology* **22:** 329–338.

Field, C., Behrenfeld, M., Randerson, J., and Falkowski, P. (1998). Primary production of the biosphere: integrating terrestrial and oceanic components. *Science* **281:** 237–240.

Finkel, Z.V. (2007). Does phytoplankton cell size matter? The evolution of modern marine food webs. *Evolution of Primary Producers in the Sea*. P.G. Falkowski and A.H. Knolls, eds. Boston, Elsevier, pp. 333–350.

Finkel, Z.V., Katz, M.E., Wright, J.D., Schofield, O.M.E., and Falkowski, P.G. (2005). Climatically-driven evolutionary change in the size of diatoms over the Cenozoic. *PNAS* **102:** 8927–8932.

Fischer, A.G. (1984). The two Phanerozoic supercycles. *Catastrophes and Earth History*. Princeton University Press, pp. 129–150.

France-Lanord, C., and Derry, L.A. (1994). $d^{13}C$ of organic carbon in the Bengal Fan: source evolution and transport of C_3 and C_4 plant carbon to marine sediments. *Geochim. Cosmochim. Acta* **58:** 4809–4814.

Gersonde, R., and Harwood, D. M. (1990). Lower Cretaceous diatoms from ODP Leg 113 Site 693 (Weddell

Sea). Part 1: vegetative cells. *Proceedings of the Ocean Drilling Program, Scientific Results*. P.F. Barker, J.P. Kennett, and S.B. O'Connell, eds. College Station TX, Ocean Drilling Program, pp. 365–402.

Gradstein, F.M., Agterberg, F.P., Ogg, J.G., Hardenbol, H., vanVeen, P., Thierry, J., and Huang, Z. (1995). A Triassic, Jurassic, and Cretaceous time scale. *Geochronology, Time Scales and Global Stratigraphic Correlations: A Unified Temporal Framework for an Historical Geology*. W.A. Berggren, D.V. Kent, and J. Hardenbol, eds. Tulsa OK, SEPM (Society for Sedimentary Geology), pp. 95–126.

Grantham, P.J., and Wakefield, L.L. (1988). Variations in the sterane carbon number distributions of marine source rock derived crude oils through geological time. *Org. Geochem*. **12:** 61–73.

Guidry, M., Arvidson, R.S., and MacKenzie, F.T. (2007). Biological and geochemical forcings to phanerozoic change in seawater, atmosphere, and carbonate precipitate composition. *Evolution of Primary Producers in the Sea*. P.G. Falkowski and A.H. Knoll, eds. Boston, Elsevier, pp. 377–403.

Hamm, C., and Smetacek, V. (2007). Armor: why, when, and how? *Evolution of Primary Producers in the Sea*. P.G. Falkowski and A.H. Knoll, eds. Boston, Elsevier, pp. 311–332.

Han, T.M., and Runnegar, B. (1992). Megascopic eukaryotic algae from the 2.1-billion-year-old Negaunee iron-formation, Michigan. *Science* **257:** 232–235.

Hansen, K.W., and Wallman, K. (2003). Cretaceous and Cenozoic evolution of seawater composition, atmospheric O_2 and CO_2: a model perspective. *Am. J. Sci*. **303:** 94–148.

Haq, B.U., Hardenbol, J., Vail, P.R. (1987). Chronology of fluctuating sea levels since the Triassic (250 million years ago) to present. *Science* **235:** 1156–1167.

Hardie, L.A. (1996). Secular variation in seawater chemistry: an explanation for the coupled secular variation in the mineralogies of marine limestones and potash evaporites over the past 600 m.y. *Geology* **24:** 279–283.

Harper, H.E., Jr., and Knoll, A.H. (1975). Silica, diatoms, and Cenozoic radiolarian evolution. *Geology* **3:** 175–177.

Harwood, D.M.M., and Gersonde, R. (1990). Lower Cretaceous diatoms from ODP Leg 113 Site 693 (Weddell Sea). Part 2: Resting spores, Chrysophycean cysts, and endoskeletal dinoflagellate, and notes on the origin of diatoms. *Proceedings of the Ocean Drilling Program.* Ocean Drilling Program, College Station, TX, pp. 403–426.

Harwood, D.M., and Nikolaev, V.A. (1995). Cretaceous diatoms: morphology, taxonomy, biostratigraphy. *Siliceous Microfossils*. C.D. Blome, P.M. Whalen, and K.M. Reed, eds. Lawrence, KS, Paleontological Society Short Courses in Paleontology, pp. 81–106.

Hayes, J., and Waldbauer, J. (2006). The carbon cycle and associated redox processes through time. *Phil Trans R. Soc. B* **361:** 931–950.

Hayes, J.M., Strauss, H., and Kaufman, A.J. (1999). The abundance of ^{13}C in marine organic matter and isotopic fractionation in the global biogeochemical cycle of carbon during the past 800 Ma. *Chem. Geol*. **161:** 103–125.

Hedges, J.I., and Keil, R.G. (1995). Sedimentary organic matter preservation: an assessment and speculative synthesis. *Mar. Chem*. **49:** 81–115.

Hodell, D.A. (1994). Magnetostratigraphic, biostratigraphic, and stable isotope stratigraphy of an Upper Miocene drill core from the Sale Briqueterie (northwestern Morocco): a high-resolution chronology for the Messinian stage. *Paleoceanography* **9:** 835–855.

Holland, H.D. (1984). *The Chemical Evolution of the Atmosphere and Oceans*. Princeton Series in Geochemistry. Princeton University Press.

Holland, H.D. (1997). Geochemistry—evidence for life on Earth more than 3850 million years ago. *Science* **275:** 38–39.

Huey, R.B., and Ward, P.D. (2005). Hypoxia, global warming, and terrestrial Late Permian extinctions. *Science* **308:** 398–401.

Ivimey-Cook, H.C. (1971). Stratigraphical palaeontology of the Lower Jurassic of the Llandbedr (Mochras Farm) Borehole. The Llandbedr (Mochras Farm) Borehole. A.W. Woodland, ed. Institute of Geological Sciences, Natural Environment Research Council, Great Britain, Report no. 71/81, p. 115.

Janis, C.M., and Damuth, J. (2000). Mammals. *Evolutionary Trends*. K.J. McNamara, ed. London, J. Belknap, pp. 301–345.

Janofske, D. (1992). Calcareous nannofossils of the Alpine Upper Triassic. *Nannoplankton Research*. B. Hamrsmid and J.R. Young, eds. Knihovnicka ZPZ, pp. 870–109.

Javaux, E.J., Knoll, A.H., and Walter, M.R. (2001). Morphological and ecological complexity in early eukaryotic ecosystems. *Nature* **412:** 66–69.

Jenkyns, H.C., and Clayton, C.J. (1997). Lower Jurassic epicontinental carbonates and mudstones from England and Wales: chemostratigraphic signals and the early Toarcian anoxic event. *Sedimentology* **44:** 687–706.

Kampschulte, A., and Strauss, H. (2004). The sulfur isotopic evolution of Phanerozoic seawater based on the analysis of structurally substituted sulfate in carbonates. *Chem. Geol*. **204:** 255–286.

Katz, M.E., Fennel, K., Berner, R.A., and Falkowski, P.G. (2005b). *Long-Term Trends in the Global Carbon Cycle: Biogeochemical Records of the Past ~200 myrs*. American Geophysical Union Ann. Mtg. abstract.

Katz, M.E., Finkel, Z.V., Grzebyk, D., Knoll, A.H., and Falkowski, P.G. (2004). Evolutionary trajectories and biogeochemical impacts of marine eukaryotic phytoplankton. *Annu. Rev. Ecol. Evol. Syst*. **35:** 523–556.

Katz, M.E., Wright, J.D., Miller, K.G., Cramer, B.S., Fennel, K., and Falkowski, P.G. (2005a). Biological overprint of the geological carbon cycle. *Mar. Geol*. **217:** 323–338.

Kidder, D.L., and Erwin, D.H. (2001). Secular distribution of biogenic silica through the Phanerozoic:

comparison of silica-replaced fossils and bedded cherts at the series level. *J. Geol*. **109:** 509–522.

Knoll, A.H. (1989). Evolution and extinction in the marine realm: some constraints imposed by phytoplankton. *Phil. Trans. R. Soc. Lond*. **325:** 279–290.

Knoll, A.H. (1992). The early evolution of eukaryotes: a geological perspective. *Science* **256:** 622–627.

Knoll, A.H. (1994). Proterozoic and Early Cambrian protists: evidence for accelerating evolutionary tempo. *Proc. Natl. Acad. Sci. USA* **91:** 6743–6750.

Knoll, A.H. (2003). *Life on a Young Planet: The First Three Billion Years of Evolution on Earth*. Princeton University Press.

Knoll, A.H., Javaux, E.J., Hewitt, D., and Cohen, P. (2006). Eukaryotic organisms in Proterozoic oceans. *Phil. Trans. R. Soc. B* **361:** 1023–1038.

Knoll, A.H., Summons, R.E., Waldbauer, J.R., and Zumberge, J.E. (2007). The geological succession of primary producers in the oceans. *Evolution of Primary Producers in the Sea*. P.G. Falkowski and A.H. Knoll, eds. Boston, Elsevier, pp. 133–163.

Kooistra, W.H.C.F., Gersonde, R., Medlin, L.K., and Mann, D.G. (2007). The origin and evolution of the diatoms: their adaptation to a planktonic existence. *Evolution of Primary Producers in the Sea*. P.G. Falkowski and A.H. Knoll, eds. Boston, Elsevier, pp. 207–249.

Kump, L.R., and Arthur, M.A. (1999). Interpreting carbon-isotope excursions: carbonates and organic matter. *Chem. Geol*. **161:** 181–198.

Laws, E.A., Falkowski, P.G., Smith, W.O., Jr., and McCarthy, J.J. (2000). Temperature effects on export production in the open ocean. *Global Biogeochem. Cycles* **14:** 1231–1246.

Lipps, J.H. (1993). *Fossil Prokaryotes and Protists*. Oxford, Blackwell, p. 342.

MacArthur, R.H. and Wilson, E.O. (1967). *The Theory of Island Biogeography*. Monographs in population biology, v. 1.

Mackenzie, F.T., and Pigott, J.D. (1981). Tectonic controls of Phanerozoic sedimentary rock cycling. *J. Geol. Soc. Lond*. **138:** 183–196.

Maldonado, M., Carmona, M.C., Uriz, M.J., and Cruzado, A. (1999). Decline in Mesozoic reef-building sponges explained by silicon limitation. *Nature* **401:** 785–788.

Maliva, R.G., Knoll, A.H., and Siever, R. (1989). Secular change in chert distribution; a reflection of evolving biological participation in the silica cycle. *Palaios* **4:** 519–532.

Martin, J., Knauer, G., Karl, D., and Broenkow, W. (1987). VERTEX: carbon cycling in the northeast Pacific. *Deep Sea Res*. **34:** 267–285.

Medlin, L.K., Kooistra, W.C.H.F., and Schmid, A.M.M. (2000). A review of the evolution of the diatoms—a total approach using molecules, morphology and geology. *The Origin and Early Evolution of the Diatoms: Fossil, Molecular and Biogeographical Approaches*. A. Witkowski and J. Sieminska, eds. Krakow, Poland, Polish Academy of Sciences, pp. 13–35.

Miller, K.G., Kominz, M.A., Browning, J.V., Wright, J.D., Mountain, G.S., Katz, M.E., Sugarman, P.J., Cramer, B.S., Christie-Blick, N., Pekar, S.F. (2005). The Phanerozoic record of global sea-level change. *Science* **310:** 1293–1298.

Moldowan, J.M., Dahl, J., Jacobson, S.R., Huizing, B.J., Fago, F.J., Shetty, R., Watts, D.S., and Peters, K.E. (1996). Chemostratigraphic reconstruction of biofacies: molecular evidence linking cyst-forming dinoflagellates with pre-Triassic ancestors. *Geology* **24:** 159–162.

Moldowan, J.M., and Jacobson, S.R. (2000). Chemical signals for early evolution of major taxa: biosignatures and taxon-specific biomarkers. *Int. Geol. Rev*. **42:** 805–812.

Moldowan, J.M., and Talyzina, N.M. (1998). Biogeochemical evidence for dinoflagellate ancestors in the Early Cambrian. *Science* **281:** 1168–1170.

Morris, I. (1987). Paths of carbon assimilation in marine phytoplankton. *Primary Productivity in the Sea*. P.G. Falkowski, ed. New York, Plenum, pp. 139–159.

Mortola, J. (2001). *Respiratory Physiology of Newborn Mammals: A Comparative Perspective*. Baltimore, Johns Hopkins University Press.

Murphy, W.J., Eizirik, E., O'Brien, J.O., Madsen, D., Scally, M., Douady, C.J., Teeling, E., Ryder, D.A., Stanhope, M.J., DeJong, W.W., and Springer, M.S. (2001). Resolution of the early placental mammal radiation using Bayesian phylogenetics. *Science* **294:** 2348–2351.

Prasad, V., Strömberg, C.A.E., Alimohammadian, H., and Sahni, A. (2005). Dinosaur coprolites and the early evolution of grasses and grazers. *Science* **310:** 1177–1180.

Premuzic, E.T. (1980). Organic carbon and nitrogen in the surface sediments of world oceans and seas: Distribution and relationship to bottom topography. *Brookhaven National Lab Formal Report* **51084**.

Racki, G. (1999). Silica-secreting biota and mass extinctions: survival patterns and processes. *Palaeogeog. Palaeoclim. Palaeoecol*. **154:** 107–132.

Ravizza, G. (1993). Variations of the $^{187}Os/^{186}Os$ ratio of seawater over the past 28 million years as inferred from metalliferous carbonates. *Ear. Planet. Sci. Lett*. **118:** 335–348.

Rea, D.K., and Ruff, L.J. (1996). Composition and mass flux of sediment entering the world's subduction zones: implications for global sediment budgets, great earthquakes, and volcanism. *Ear. Planet. Sci. Lett*. **140:** 1–12.

Reinfelder, J.R., Kraepeil, A.M.L., and Morel, F.M.M. (2000). Unicellular C_4 photosynthesis in a marine diatom. *Nature* **407:** 996–999.

Retallack, G.J. (1997). Cenozoic expansion of grasslands and climatic cooling. *J. Geol*. **109:** 407–426.

Retallack, G.J. (2001). Neogene expansion of the North American prairie. *Palaios* **12:** 380–390.

Rich, J.E., Johnson, G.L., Jones, J.E., and Campsie, J. (1986). A significant correlation between fluctuations in seafloor spreading rates and evolutionary pulsations. *Paleoceanography* **1:** 85–95.

Roman, M.R., Adolf, H.A., Landry, M.R., Madin, L.P., Steinberg, D.K., and Zhang, X. (2002). Estimates of oceanic mesozooplankton production: a comparison using the Bermuda and Hawaii time-series data. *Deep Sea Res. Part II Top. Studies Oceanogr*. **49:** 175–192.

Ronov, A.B. (1994). Phanerozoic transgressions and regressions on the continents: a quantitative approach based on areas flooded by the sea and areas of marine and continental deposition. *Am. J. Sci.* **294:** 777–801.

Rosenweig, M.L. (1995). *Species Diversity in Space and Time*. Cambridge, CUP.

Rothpletz, A. (1896). Über die flysch-fucoiden und einige andere fossile Algen, sowie über liasische, diatomeen fuhrende Hornschwamme. *Zeitschrift Deutsch Geolog. Gesellschaft* **48:** 854–914.

Royer, D., Berner, R. A., Montanez, I.P., Tabor, N.J., and Beerling, D.J. (2004). CO_2 as a primary driver of Phanerozoic climate. *GSA Today* **14:** 4–10.

Sancetta, C., Villareal, T., and Falkowski, P.G. (1991). Massive fluxes of rhizosolenoid diatoms: A common occurrence? *Limnol. Oceanogr*. **36:** 1452–1457.

Sandberg, P.A. (1975). New interpretations of Great Salt Lake ooids and of ancient nonskeletal carbonate mineralogy. *Sedimentoloty* **22:** 497–538.

Schmidt-Nielson, K. (1970). Energy metabolism, body size, and problems of scaling. *Fed. Proc*. **29:** 1524–1532.

Schrag, D.P. (2002). *Control of Atmospheric CO_2 and Climate over the Phanerozoic American Geophysical Union*, Fall Meeting abstract.

Shackleton, N.J. (1987). Oxygen isotopes, ice volume, and sea level. *Q. Sci. Rev*. **6:** 183–190.

Shackleton, N.J., and Hall, M.A. (1984). Carbon isotope data from Leg 74 sediments. *Init. Repts. DSDP*. T.C. Moore, Jr., P.D. Rabinowitz, eds. Washington DC, U.S. Government Printing Office, pp. 613–619.

Shanks, A., and Trent, J. (1980). Marine snow: sinking rates and potential role in vertical flux. *Deep Sea Res*. **27:** 137–143.

Shine, R. (2005). Life-history evolution in reptiles. *Annu. Rev. Ecol. Evol. Syst*. **36:** 23–46.

Sibley, D.F., and Vogel, T.A. (1976). Chemical Mass Balance of the Earth's crust: the calcium dilemma (?) and the role of pelagic sediments. *Science* **192:** 551–553.

Smayda, T.J. (1969). Some measurements of the sinking rate of fecal pellets. *Limnol. Oceanogr*. **14:** 621–625.

Smayda, T.J. (1970). The suspension and sinking of phytoplankton in the sea. *Oceanogr. Mar. Bio. Annu. Rev*. **8:** 353–414.

Smetacek, V. (1999). Diatoms and the ocean carbon cycle. *Protist* **150:** 25–32.

Smith, A.B., Gale, A.S., and Monks, N.E.A. (2001). Sea-level change and rock-record bias in the Cretaceous: a problem for extinction and biodiversity studies. *Paleobiology* **27:** 241–253.

Southam, J.R., and Hay, W.W. (1981). Global sedimentary mass balance and sea level changes. *The Sea*. C. Emiliani, ed. New York, Wiley-Interscience, pp. 1617–1684.

Spencer-Cervato, C. (1999). The Cenozoic deep sea microfossil record: explorations of the DSDP/ODP sample set using the Neptune database. *Palaeontol. Electronica* **2:** 1–270.

Springer, M.S., Murphy, W.J., Eizirik, E., and O'Brien, S.J. (2003a). Placental mammal diversification and the Cretaceous-Tertiary boundary. *Proc. Nat. Acad. Sci. USA* **100:** 1056–1061.

Stanley, G.D., Jr. and Hardie, L.A. (1998). Secular oscillations in the carbonate mineralogy of reef-building and sediment-producing organisms driven by tectonically forced shifts in seawater chemistry. *Palaeogeogr. Palaeoclimatol. Palaeoecol*. **144:** 3–19.

Still, C.J., Berry, J.A., Collatz, G.J., and DeFries, R.S. (2003). Global distribution of C_3 and C_4 vegetation: carbon cycle implications. *Glob. Biogeochem. Cycles* **17**:doi:1029/2001GB001807.

Stover, L.E., Brinkhuis, H., Damassa, S.P. *et al*. (1996). Mesozoic-Tertiary dinoflagellates, acritarchs & prasinophytes. *Palynology: Principles and Applications*. J. Jansonius and D.C. McGregor, eds. Amer. Assoc. Strat. Palynologists Foundation, pp. 641–750.

Summons, R., Jahnke, L., Hope, J., and Logan, G. (1999). 2-Methylhopanoids as biomarkers for cyanobacterial oxygenic photosynthesis. *Nature* **400:** 554–557.

Summons, R.E., Thomas, J., Maxwell, J.R., and Boreham, C.J. (1992). Secular and environmental constraints on the occurrence of dinosterane in sediments. *Geochim. Cosmochim. Acta* **56:** 2437–2444.

Summons, R.E., and Walter, M.R. (1990). Molecular fossils and microfossils of prokaryotes and protists from Proterozoic sediments. *Am. J. Sci*. **290–A:** 212–244.

Tappan, H. (1974). Molecular oxygen and evolution. *Molecular Oxygen in Biology: Topics in Molecular Oxygen Research*. O. Hayaishi, ed. Amsterdam, North-Holland Publishing Company, pp. 81–135.

Tappan, H. (1980). *The Palaeobiology of Plant Protists*. San Francisco, W.H. Freeman, pp. 1028.

Tappan, H., and Loeblich, J. (1988). Foraminiferal evolution, diversification, and extinction. *J. Paleontol*. **62:** 695–714.

Treguer, P., Nelson, D.M., van Bennekom, A.J., DeMaster, D.J., Leynaert, A., and Queguiner, B. (1995). The silica balance in the world ocean: a reestimate. *Science* **268:** 375–379.

Turekian, K.K., and Pegram, W.J. (1997). Os isotope record in a Cenozoic deep-sea core: its relation to global tectonics and climate. *Tectonic Uplift and Climate Change*. W.F. Ruddiman, ed. New York, Plenum Press, pp. 383–397.

Urrere, M., and Knauer, G. (1981). Zooplankton fecal pellet fluxes and vertical transport of particulate organic material in the pelagic environment. *J. Plankton Res*. **3:** 369–387.

Vail, P.R., Mitchum, R.M., Todd, R.G., Widmier, J.M., Thompson III, S. Sangree, J.B., Bubb, J.N., and Hatelid, W.G. (1977). Seismic Stratigraphy and global changes of sea level. *Seismic Stratigraphic—Applications of Hydrocarbon Exploration*. C.E. Payton, Memoirs of the American Association of Petroleum Geologists. **26:** 49–205.

Valentine, J.W., and Moores, E.M. (1974). Plate tectonics and the history of life in the oceans. *Sci. Am*. **230:** 80–89.

van Andel, T.H. (1975). Mesozoic/Cenozoic calcite compensation depth and global distribution of calcareous sediments. *Earth Planetary Sci. Lett*. **26:** 187–194.

Veizer, J., Ala, K., Azmy, K., Brunckschen, P., Buhl, D., Bruhn, F., Carden, G.A.F., Diener, A., Ebneth, S., Godderis, Y., Jasper, T., Korte, C. Pawallek, F., Podlaha, O.G., and Strauss, H. (1999). $^{87}Sr/^{86}Sr$, $\delta^{13}C$, and $\delta^{18}O$ evolution of Phanerozoic seawater. *Chem. Geol*. **161:** 59–88.

Vincent, E., and Berger, W.H. (1985). Carbon dioxide and polar cooling in the Miocene: the Monterey hypothesis. *The Carbon Cycle and Atmospheric CO2: Natural Variations Archean to Present*. Geophys. Monogr. E.T. Sundquist and W.S. Broecker, eds. Washington DC, AGU, pp. 455–468.

Volk, T., and Hoffert, M.I. (1985). Ocean carbon pumps: Analysis of relative strengths and efficiencies in ocean-driven atmospheric CO_2 changes. *Geophys. Monogr*. **32:** 99–110.

Walker, L.J., Wilkinson, B.H., and Ivany, L.C. (2002). Continental drift and Phanerozoic carbonate accumulation in shallow-shelf and deep-marine settings. *J. Geol*. **110:** 75–87.

Wallman, K. (2001). Controls on the Cretaceous and Cenozoic evolution of seawater composition, atmospheric CO_2 and climate. *Geochim. Cosmochim. Acta* **65:** 3005–3025.

Walsh, J.J. (1988). *On the Nature of Continental Shelves*. San Diego, Academic Press.

Weibel, E.R., and Hoppeler, H. (2005). Exercise-induced maximal metabolic rate scales with muscle aerobic capacity. *J Exp. Biol*. **208:** 1635–1644.

Whitfield, M. (2001). Interactions between phytoplankton and trace metals in the ocean. *Adv. Mar. Biol*. **41:** 3–128.

Wilkinson, B.H., and Algeo, T.J. (1989). Sedimentary carbonate record of calcium-magnesium cycling. *Am. J. Sci*. **289:** 1158–1194.

Wilson, J.T. (1966). Did the Atlantic close and then re-open? *Nature* **211:** 676–681.

Wing, S.L., Sues, H.D., Potts, R., DiMichele, W.A., and Behrensmeyer, A.K. (1992). Evolutionary paleoecology. *Terrestrial Ecosystems Through Time: Evolutionary Paleoecology of Terrestrial Plants and Animals*. A.K. Behrensmeyer, J. Damuth, W.A. DiMichele, R. Potts, H.D. Sues, and S.L. Wing, eds. Chicago, University of Chicago Press, pp. 1–14.

Woodland, A.W. (1971). The Llanbedr (Mochras Farm) Borehole. Institute of Geological Sciences, Natural Environment Research Council, Great Britain, Report no. 71/81, p. 115.

Worsley, T.R., and Nance, R.D. (1989). Carbon redox and climate control through Earth history: a speculative reconstruction. *Palaeogeogr. Palaeoclimatol. Palaeoecol*. **75:** 259–282.

Worsley, T.R., Nance, R.D., and Moody, J.B. (1986). Tectonic cycles and the history of the Earth's biogeochemical and paleoceanographic record. *Paleoceanography* **1:** 233–263.

Zhang, Z. (1986). Clastic facies microfossils from the Chuanlingguo Formation near Jixian, North China. *J. Micropaleontol*. **5:** 9–16.